Ultrasound of Common Vascular Lesions

4

Ximena Wortsman

Contents

The 2014 update of the classification of vascular anomalies performed by the International Society for the Study of Vascular Anomalies (ISSVA) [1] separates the vascular anomalies into two major groups: vascular tumors and vascular malformations. Within these groups, vascular tumors can be divided into benign, borderline, and malignant types. Vascular malformations are classified as simple, combined, malformations of major named vessels, and malformations associated with other anomalies. Nevertheless, there are some non-classified vascular entities (usually less frequent), such as angiokeratoma, verrucous hemangioma, multifocal lymphangioendotheliomatosis with thrombocytopenia (MLT), cutaneovisceral angiomatosis with thrombocytopenia (CAT), kaposiform lymphangiomatosis, and PTEN-type hamartoma of the soft tissue [1–8]. This chapter reviews the most common vascular conditions.

4.1 Vascular Tumors

Vascular tumors are characterized by endothelial proliferation and can be separated into benign, locally aggressive/borderline, or maligvnant tumors. Of these, the most frequent are benign vascular tumors, which include infantile hemangioma, congenital hemangioma, reactive proliferative vascular lesions, and other vascular tumors [1–3].

4.1.1 Infantile Hemangioma (IH)

4.1.1.1 Definition

Infantile hemangioma (IH) is a benign endothelial cell proliferation positive for glucose transporter 1 (GLUT-1). IH is the most common tumor of infancy and accounts for up to 5% of all tumors. Clinically, these tumors initially present a phase characterized by fast growth after birth, also called proliferative phase.

Electronic supplementary material The online version of this chapter (https://doi.org/10.1007/978-3-319-89614-4_4) contains supplementary material, which is available to authorized users.

X. Wortsman, *Atlas of Dermatologic Ultrasound*, https://doi.org/10.1007/978-3-319-89614-4_4

Then, they show a plateau, and later, they start phases of partial and total (or almost total) regression or involution [2–8].

4.1.1.2 Synonym

Hemangioma of infancy.

4.1.1.3 IH Classification

IH can be classified according to:

Pattern of distribution:

- focal
- multifocal
- segmental
- indeterminate

Layers of involvement:

- dermal, also called superficial IH
- hypodermal and/or deeper layer, also called deep IH
- mixed forms (dermal-superficial and hypodermal-deep)

4.1.1.4 Associated Syndromes

IH, particularly when they present as large and segmental variants, can be associated with other vascular and non-vascular anomalies, including some well-known syndromes [2–8]:

- *PHACE syndrome* (posterior fossa brain malformations, hemangiomas, arterial anomalies, cardiovascular defects, and eye anomalies, with or without midline ventral defects such as sternal clefting or supraumbilical raphe)
- *LUMBAR syndrome* (lower body hemangioma, urogenital anomalies/ulceration, myopathy, bony deformities, anorectal or arterial anomalies, and renal anomalies)

4.1.1.5 Key Sonographic Signs

The ultrasonographic appearance (echogenicity and degree of vascularity) of IH varies according to the phase of the lesion (Fig. 4.1) [9–16]. The proliferative and partial regression phases are considered active stages of proliferation, with differences in the degree of the vascularity [11–13].

Proliferative Phase

- Ill-defined, hypoechoic, hypervascular solid, mass-like structure
- Spectral curve analysis shows arterial and venous vessels, and sometimes arteriovenous shunts.
- Occasionally, IH can show direct afferent branches from medium-size arteries that would be important to describe.
- It is relevant to report the thickness and layers of involvement of the hemangioma (Figs. 4.2, 4.3, and 4.4; Videos 4.1, 4.2, and 4.3).

Partial Regression Phase

Ill-defined, heterogeneous, solid mass-like structure with a mixed pattern of vascularity that presents hypervascular and hypovascular areas (Fig. 4.5; Video 4.4).

Total Regression Phase

- Ill-defined structure that is hypovascular or without detectable vascularity. The hypodermis is usually hyperechoic in sites affected by the hemangioma, but focal areas of thinning of the dermis and hypertrophic hypodermal lipodystrophy may be also detected (Fig. 4.6).
- The appearance of this phase may vary according to the type of treatment that the patient has received before the ultrasound examination. For example, lesions that have been treated with steroids tend to show more atrophy signs. Lesions that have been partially removed by surgery may present hypoechoic scarring tissue, sometimes with a laminar pattern and/or areas with distorted heterogeneous architecture (Fig. 4.7).

4.1.1.6 Tips

- If more than five cutaneous hemangiomas are present, it is recommended to extend the examination and to scan the liver in order to look for hepatic hemangiomas.
- In children younger than 6 months with midline lesions, it is suggested to extend the examination and scan the brain and spinal cord. In older children, the scanning of the brain will depend on the size of the anterior fontanel (the site used for accessing the brain on ultrasound), which usually closes around 1 year of age.
- The scanning of the spinal cord will depend on the degree of ossification of the spine, which normally increases in children older than 6 months. Therefore, keep in mind that ultrasound can allow studying the spinal cord in children younger than 6 months.
- In older children, the brain and spinal cord cannot be fully displayed on ultrasound because the normal calcification of the skull and spine stops the soundwaves.

4.1.2 Congenital Hemangioma

4.1.2.1 Definition

Congenital hemangioma (CH) is a proliferative endothelial cell proliferation that is usually present at birth and is negative for glucose transporter 1 (GLUT-1). CHs are less common than IHs.

4.1.2.2 Classification

CHs can be classified according to their evolution [12, 17–19]:

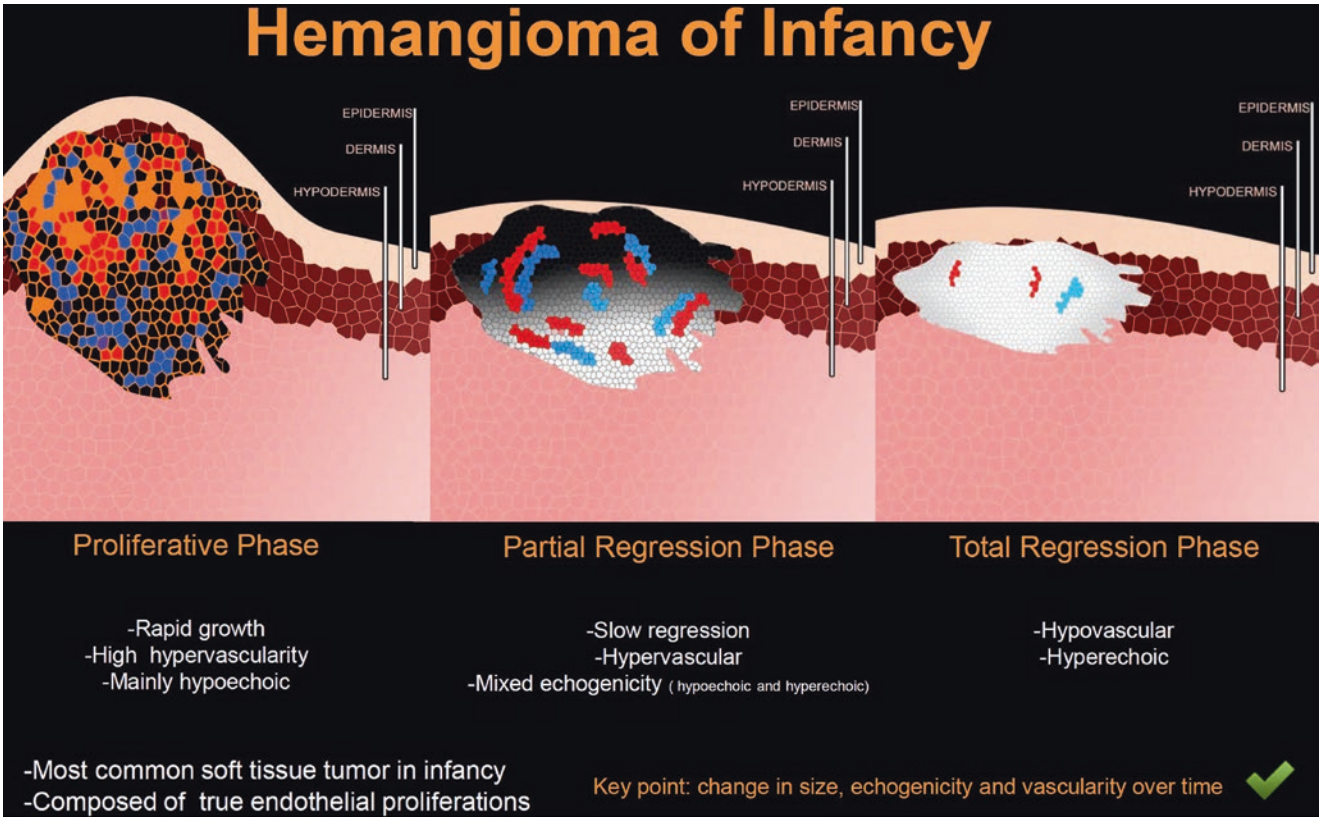

Fig. 4.1 Phases of infantile hemangioma.

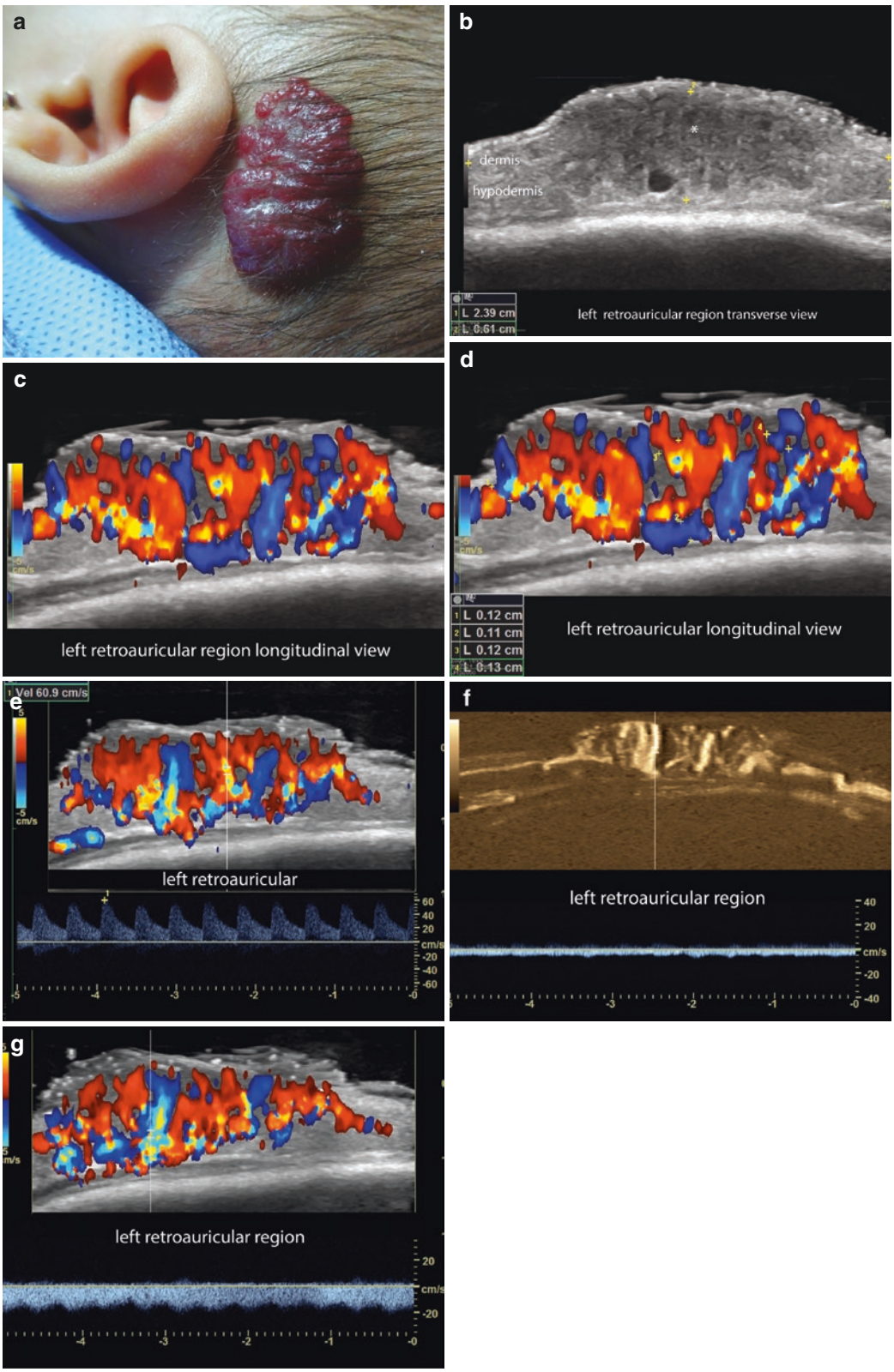

Fig. 4.2 Infantile hemangioma in proliferative phase, with sequence that shows a summary of the protocol for studying hemangiomas. (**a**) Clinical image of the lesion in the left retroauricular region. (**b**) Greyscale ultrasound (transverse view). (**c** and **d**) Color Doppler ultrasound shows the vessels (**c**) and their thicknesses (**d**) within the lesion. (**e** and **g**) Color Doppler ultrasound with spectral curves analyses. (**f**) Echoangiogram (B-flow, General Electric Health Systems; Milwaukee, WI, USA) that demonstrates the type of the flow. The child presented a 2.39-cm (transverse) × 0.61-cm (thickness), ill-defined dermal and hypodermal hypoechoic solid structure(*) with a mass-like appearance (**b**). There is a diffuse, prominent hypervascularity in the structure (**c**), and thickness of the lesional vessels varies between 1.1 and 1.3 mm (**d**). Notice the presence of high peak systolic velocity in the arterial vessels that reaches 60 cm/s (**e**), the monophasic venous flow in (**f**), and the arterialized venous flow in (**g**). See Video 4.1.

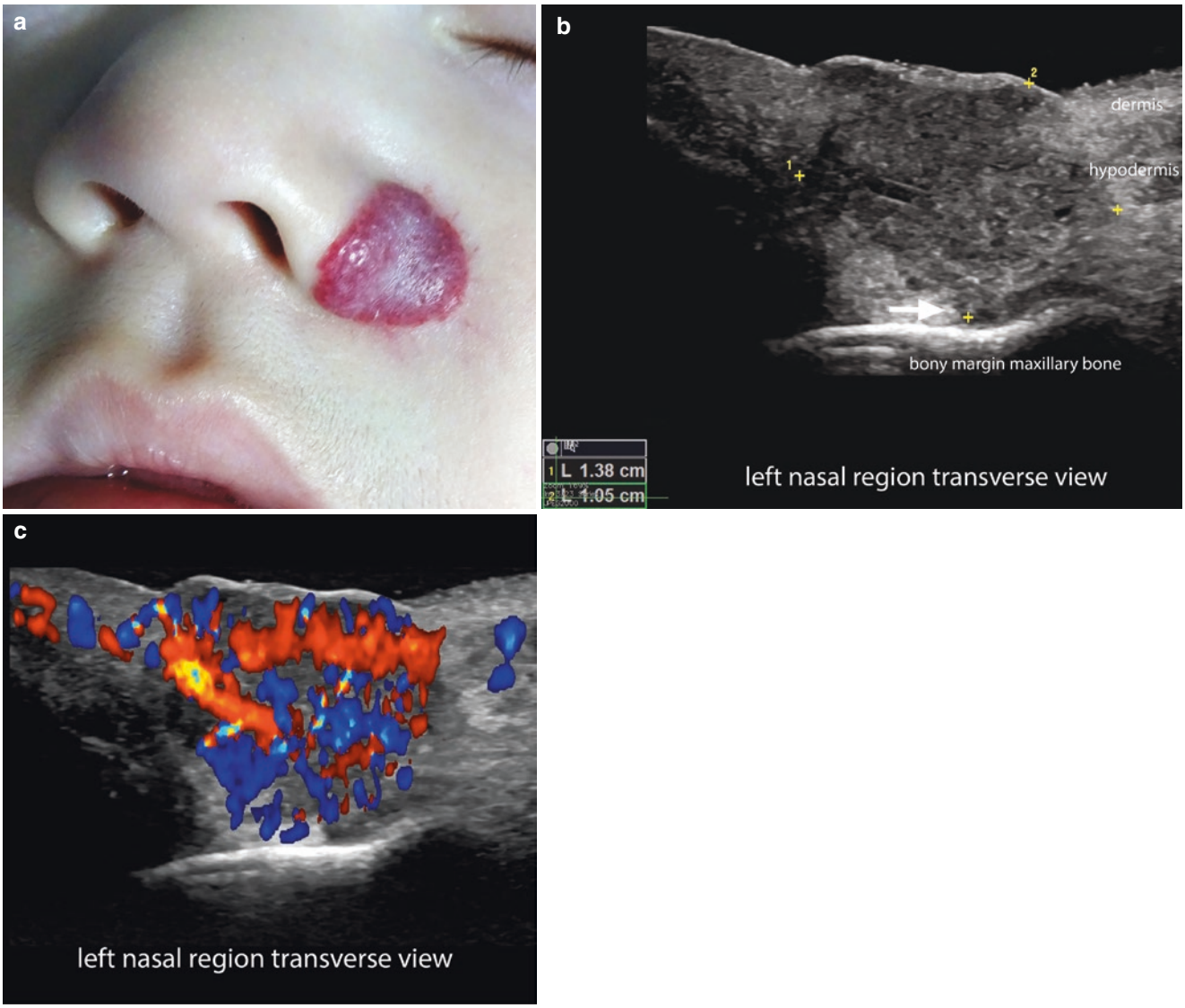

Fig. 4.3 Hemangioma in proliferative phase. (**a**) Clinical photograph of the lesion in the left nasal and perinasal region. (**b** and **c**) Greyscale and color Doppler ultrasound (transverse views; left nasal region) shows a 1.38-cm (transverse) × 1.05-cm (thickness), ill-defined, hypoechoic structure in the dermal and hypodermal layers. In the lateral border (right side of the image; *arrow* in b) the lesion involves the muscle and contacts the bony margin of the left maxilla. The color Doppler shows prominent hypervascularity in all the parts of the lesion in (**c**). See Video 4.2.

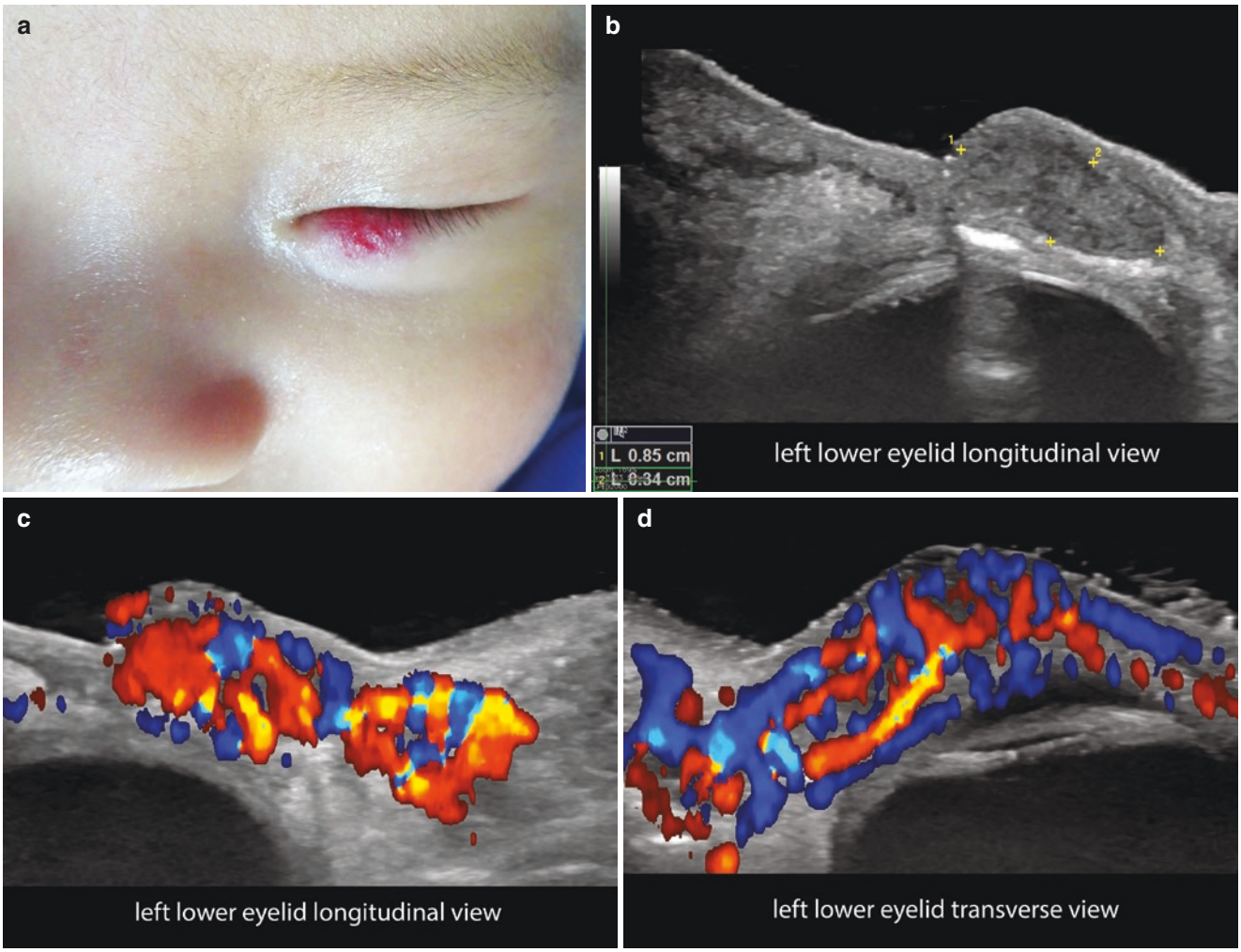

Fig. 4.4 Hemangioma in proliferative phase. (**a**) Clinical image of the lesion in the lower eyelid. (**b**–**d**) Greyscale and color Doppler ultrasound (**c**, longitudinal view; **d**, transverse view) demonstrate an ill-defined hypoechoic structure (between markers), 8.5 mm (length) × 3.4 mm (thickness) that involves the orbicularis muscle of the lower eyelid. Notice the diffuse hypervascularity that involves dermis, the orbicularis muscle, and the posterior aspect of the lower eyelid (**c** and **d**). In (**c**) involvement of the dermis and hypodermis of the upper part of the of the cheek is detected. See Video 4.3.

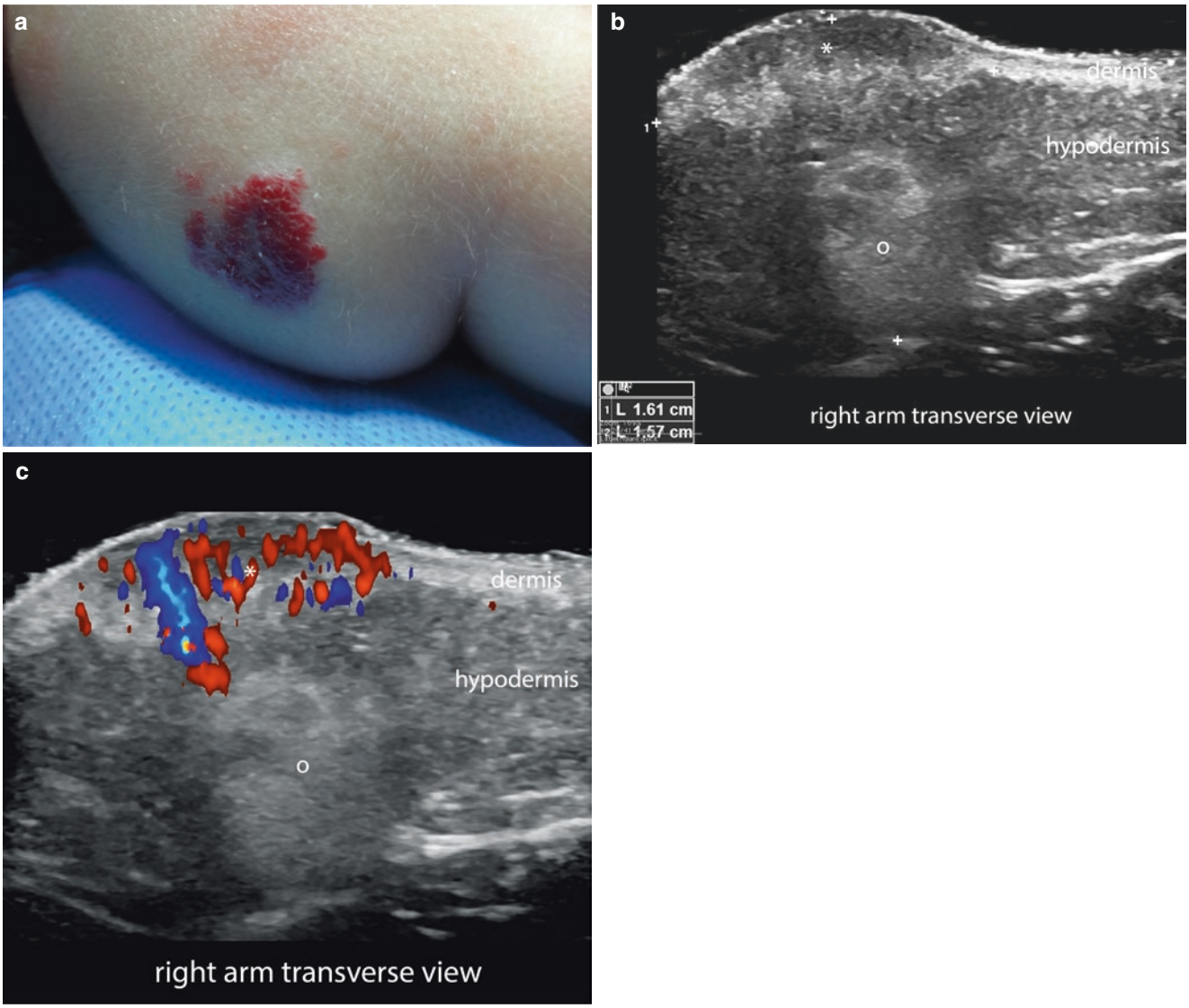

Fig. 4.5 Hemangioma in partial regression phase. (**a**) Clinical photograph of a bulging lesion in the right arm of a 10 month-old baby. (**b** and **c**) Greyscale and color Doppler ultrasound (transverse views; right arm) show 1.6-cm (transverse) × 1.6-cm (thickness), ill-defined dermal and hypodermal bulging structure with thickening of the dermis and a mass-like appearance. The superficial part (*asterisk*) is mainly hypoechoic, and the deep part (*o*) is predominantly hyperechoic. On color Doppler (**c**), there is hypervascularity in the superficial part (proliferative phase) and hypovascularity in the deep part (regression phase). See Video 4.4.

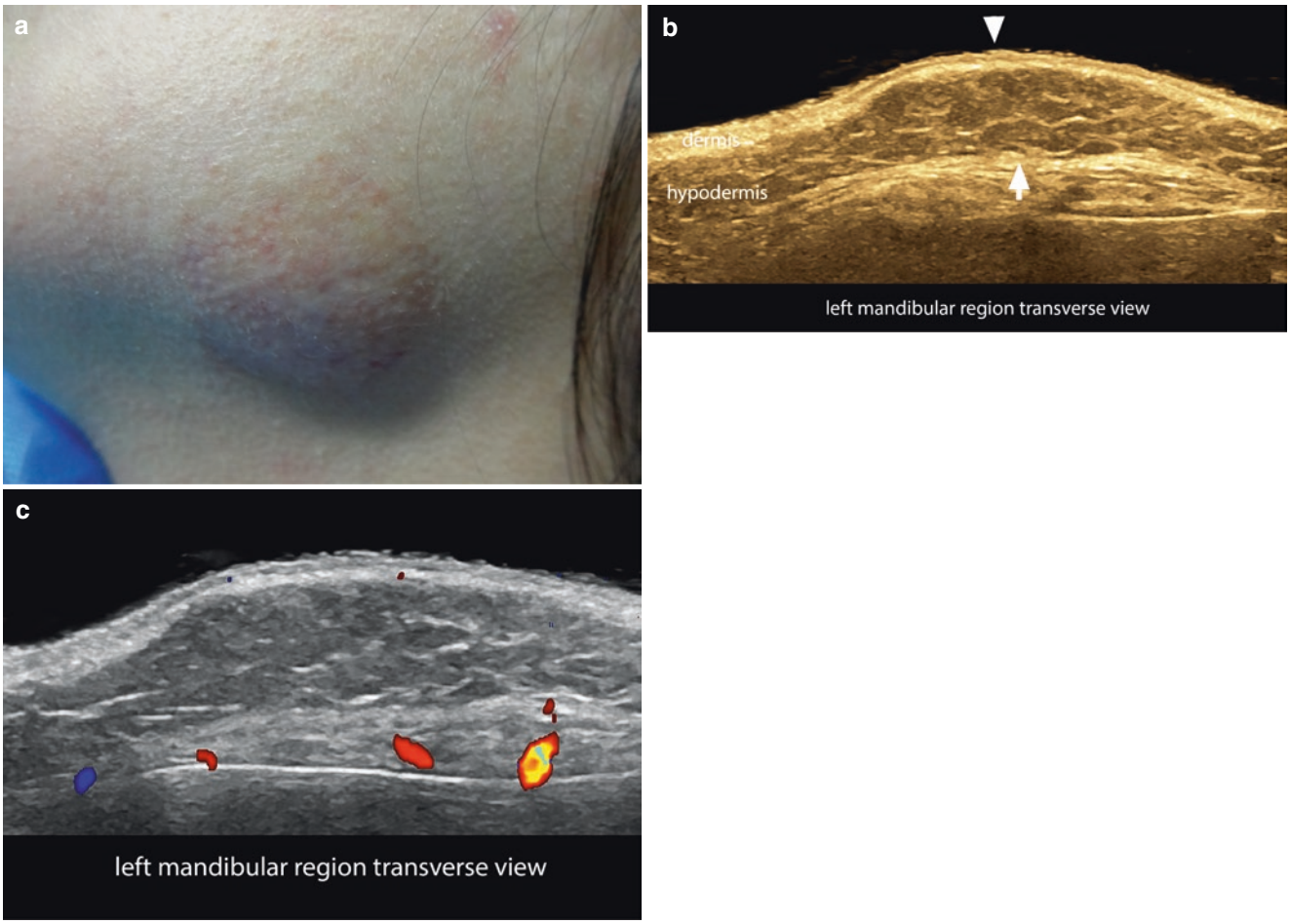

Fig. 4.6 Hemangioma in total regression phase with residual atrophic dermis and a hypertrophic hypodermal lipodystrophy. (**a**) Clinical image of the lesion in the left mandibular region. (**b** and **c**) Greyscale (with color filter) and color Doppler ultrasound (transverse views; left mandibular region) demonstrate a focal area (*arrows*) with decreased dermal thickness and increased thickness of the fatty hypodermal component (hypertrophic lipodystrophy). This focal site presents hypovascularity on color Doppler (**c**).

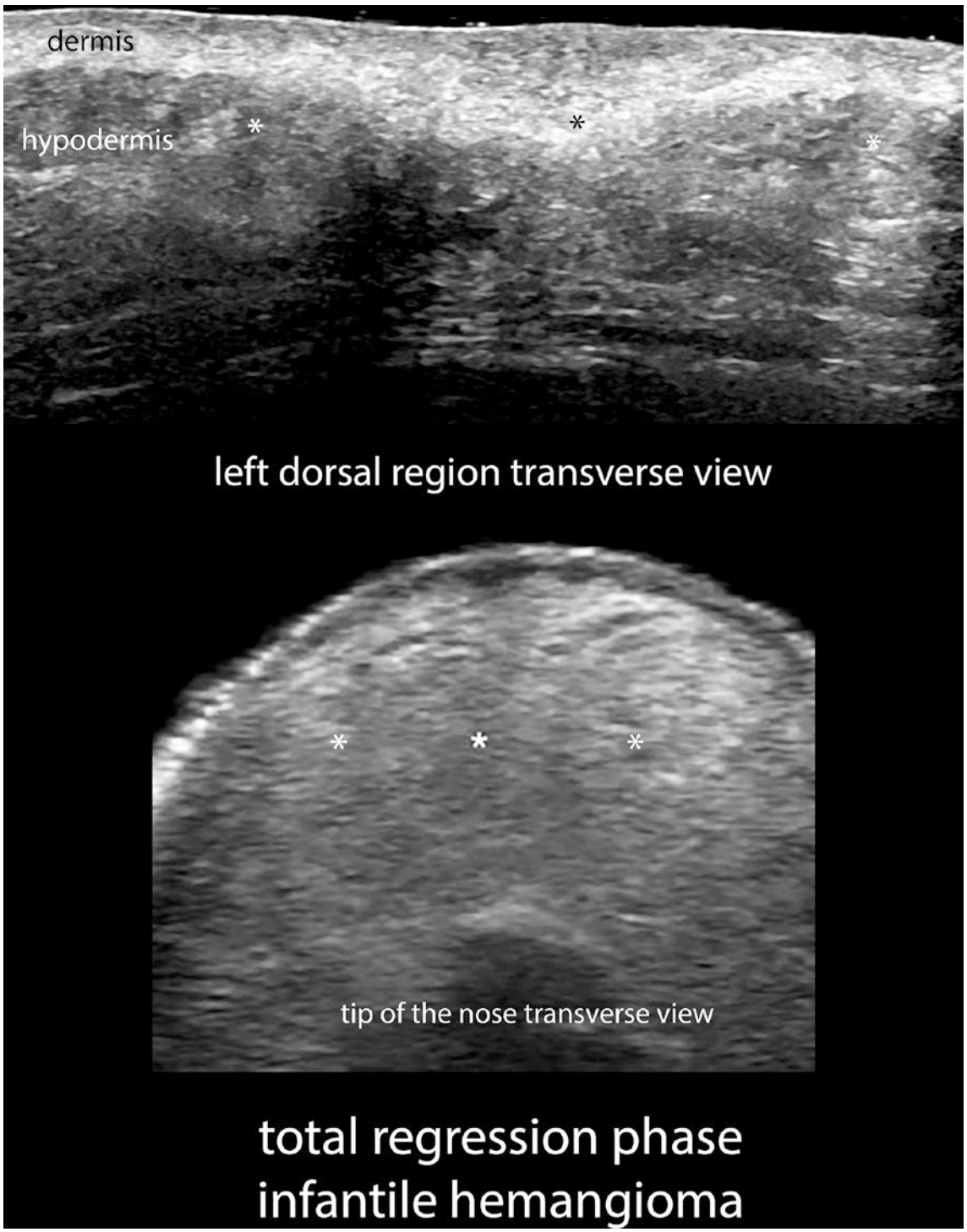

Fig. 4.7 Hemangiomas in total regression phase with hyperechoic pattern. Ultrasound Greyscale (transverse views). On top (dorsal region), the residual dermal and hypodermal fibrofatty tissue (*asterisks*) is associated with scarring and distortion of the architecture in the center of the lesion. These findings are due to an intent of partial resection of the hemangioma. At the bottom (nasal region), the residual fibrofatty tissue (*asterisks*) involves dermis, hypodermis, and the region of both alar nasal cartilages (no cartilage is detected). This can be critical information in case of a reparative surgery.

- Rapidly involuting congenital hemangioma (RICH), which supposedly regresses during the first 6–18 months of life
- Non-involuting congenital hemangioma (NICH), which does not regress spontaneously
- Partially involuting congenital hemangiomas (PICH), which present an initial involution and then a partial regression.

4.1.2.3 Key Sonographic Signs

Rapidly Involuting Congenital Hemangioma (RICH)

- At birth, these hemangiomas appear as ill-defined or well-defined hypoechoic structures affecting dermis and commonly hypodermis and deeper layers. RICHs present high vascularity with arterial and venous vessels; venous vessels are usually more prominent than in IH.
- In contrast with infantile hemangiomas, RICHs tend to show a fast and spontaneous decrease in size, increase in echogenicity, and decrease in vascularity after birth. This spontaneous involution process usually takes place during the first year of life (Figs. 4.8, 4.9, and 4.10; Videos 4.5, 4.6, and 4.7).

Non-involuting Congenital Hemangioma (NICH)

These are similar to RICH in sonographic appearance, but they may show even more dilatation of the venous component and sometimes can present hyperechoic, calcified deposits (Figs. 4.11 and 4.12; Videos 4.8 and 4.9).

- In some cases, direct feeding branches from the main arteries can be detected.
- NICHs tend to maintain their ultrasound characteristics, particularly their size, and do not regress over time. However, in some cases they may become more heterogeneous.

Partially Involuting Congenital Hemangioma (PICH)

- These have an ultrasound appearance similar to the previous types. They can present partial signs of regression, such as some decrease in size and vascularity, but PICHs do not fully regress.
- In some cases, direct feeding branches from the main arteries can be detected.

4.1.3 Telangiectatic Granuloma

4.1.3.1 Definition

Benign reactive endothelial vascular proliferation that can involve the skin and the mucosa and has been related to trauma, chronic irritation, drugs, and hormones. It is more common in females and in the face, but it can also affect other locations such as the finger, including the ungual and periungual regions. This tumor frequently presents a fast growth and tends to show bleeding and ulceration. The most common tumor of this type is the telangiectatic granuloma [12, 20, 21].

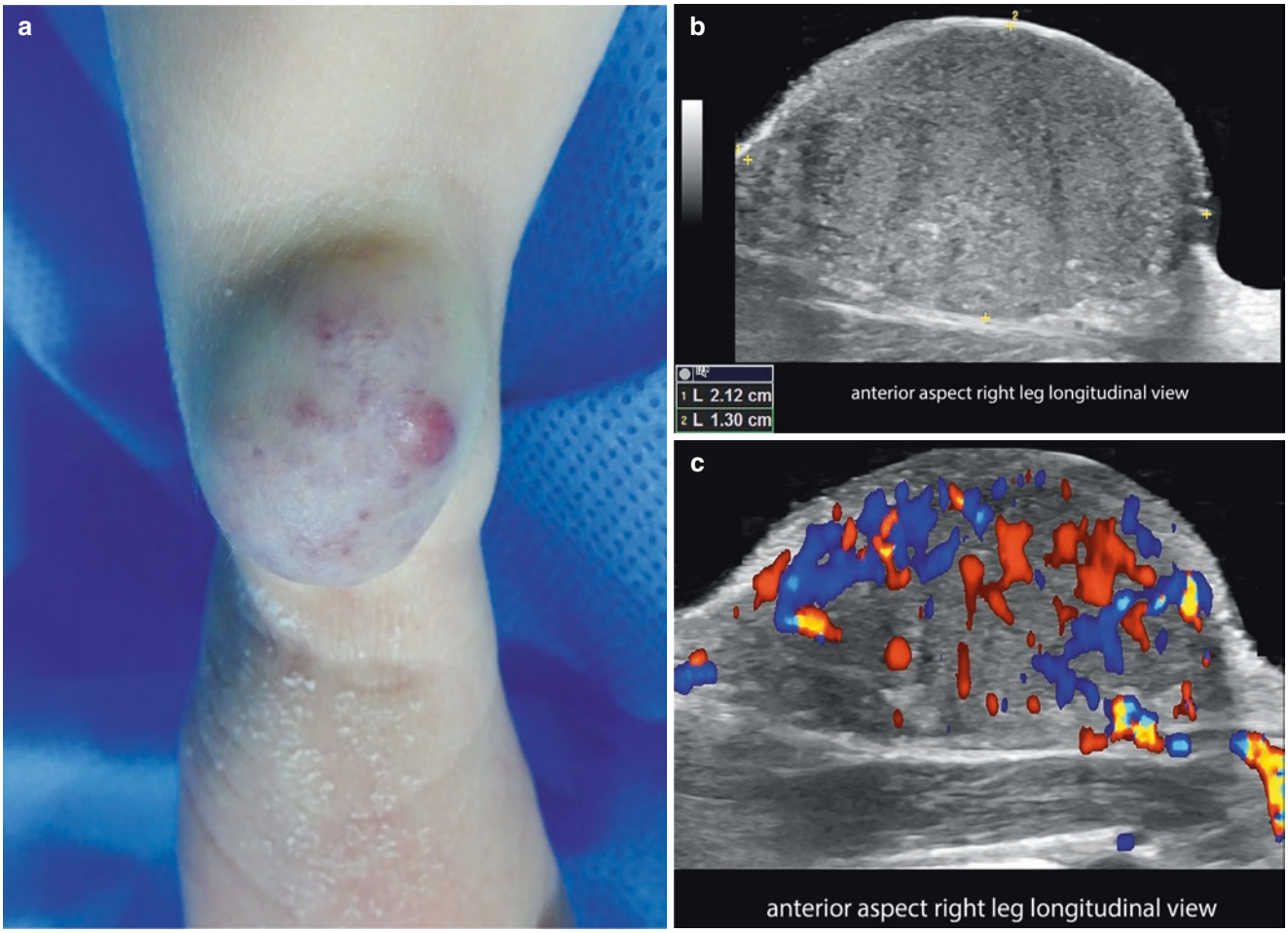

Fig. 4.8 Rapidly involuting congenital hemangioma (RICH). Basal study in a 1-month-old child. (**a**) Clinical image (anterior aspect of the distal part of the right leg). (**b** and **c**) Greyscale and color Doppler ultrasound (longitudinal views) demonstrates 2.1-cm (long) × 1.3-cm (thickness) hypoechoic dermal and hypodermal solid mass-like structure (between markers). On color Doppler (**c**), there is prominent vascularity within the lesion. See Video 4.5.

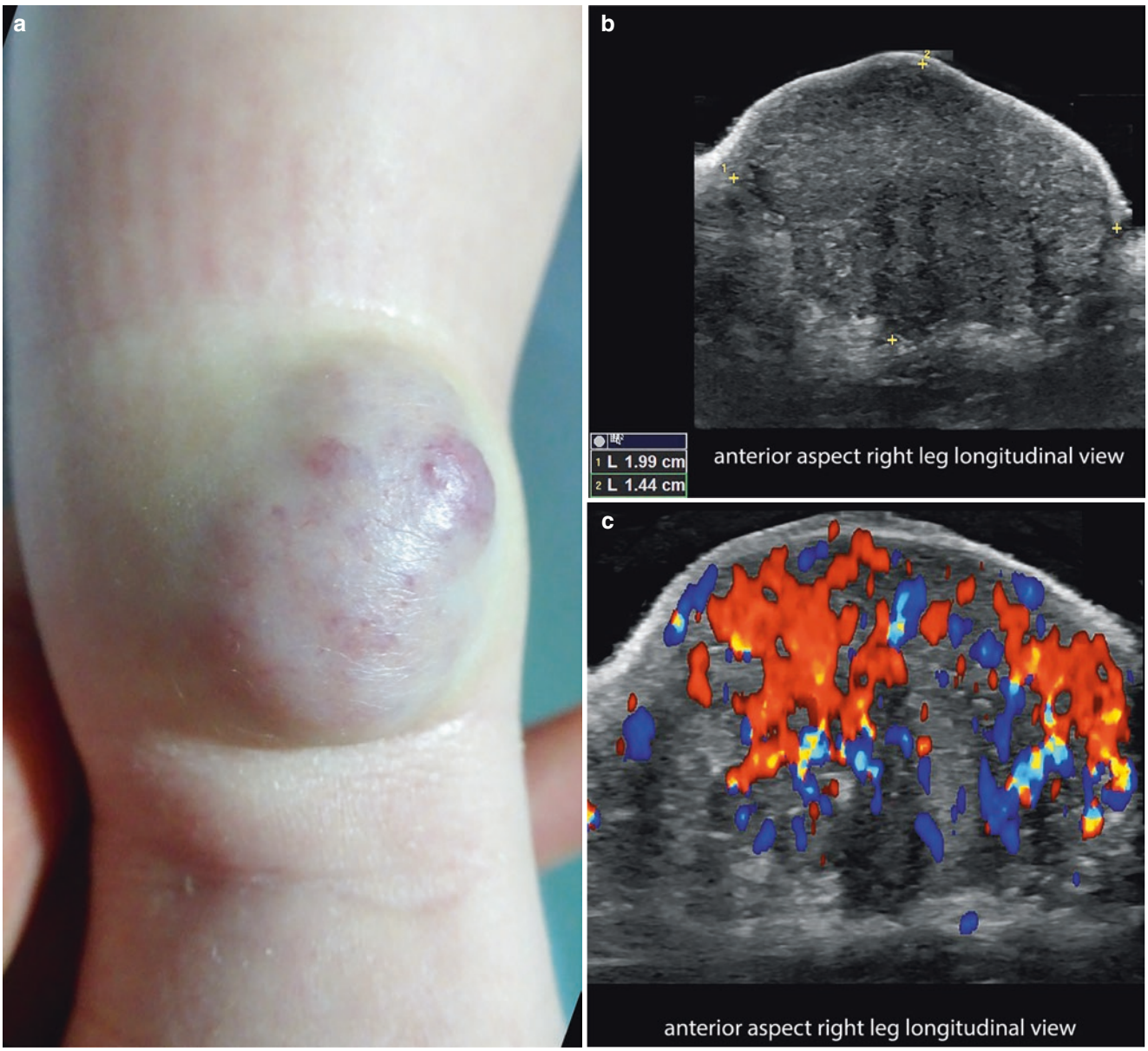

Fig. 4.9 Rapidly involuting congenital hemangioma (RICH). 3-month follow-up of the same case as in Fig. 4.8, which has been under observation and without medication. (**a**) Clinical image (anterior aspect of the distal part of the right leg). (**b** and **c**) Greyscale and color Doppler ultrasound (longitudinal views) demonstrates 2.0-cm (long) × 1.4-cm (thickness) hypoechoic dermal and hypodermal mass-like structure. Notice that the lesion is becoming more hyperechoic in the periphery of the mass and that the size is similar to the basal study; color Doppler (**c**) still shows prominent vascularity within the mass. See Video 4.6.

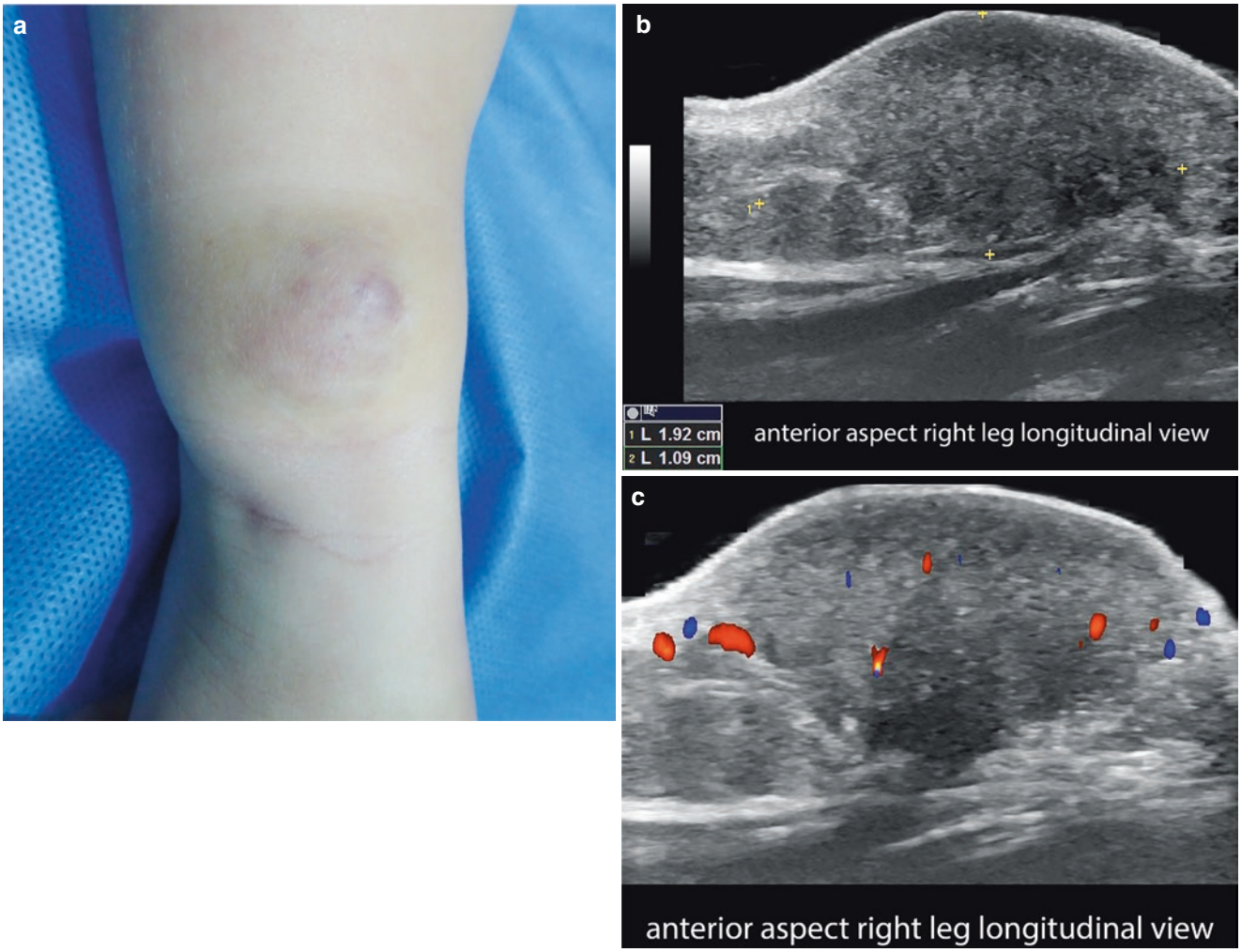

Fig. 4.10 Rapidly involuting congenital hemangioma (RICH). 6-month follow-up of the same case, which has been under observation and without medication. (**a**) Clinical image (anterior aspect of the distal part of the right leg). (**b** and **c**) Greyscale and color Doppler ultrasound (longitudinal views) demonstrates 1.9-cm (long) × 1.0-cm (thickness) more ill-defined dermal and hypodermal mass-like structure. The lesion is slightly more hyperechoic and heterogeneous than in the previous studies, and there is a small decrease in the thickness. Color Doppler (**c**) shows a significant decrease of the vascularity within the mass. See Video 4.7.

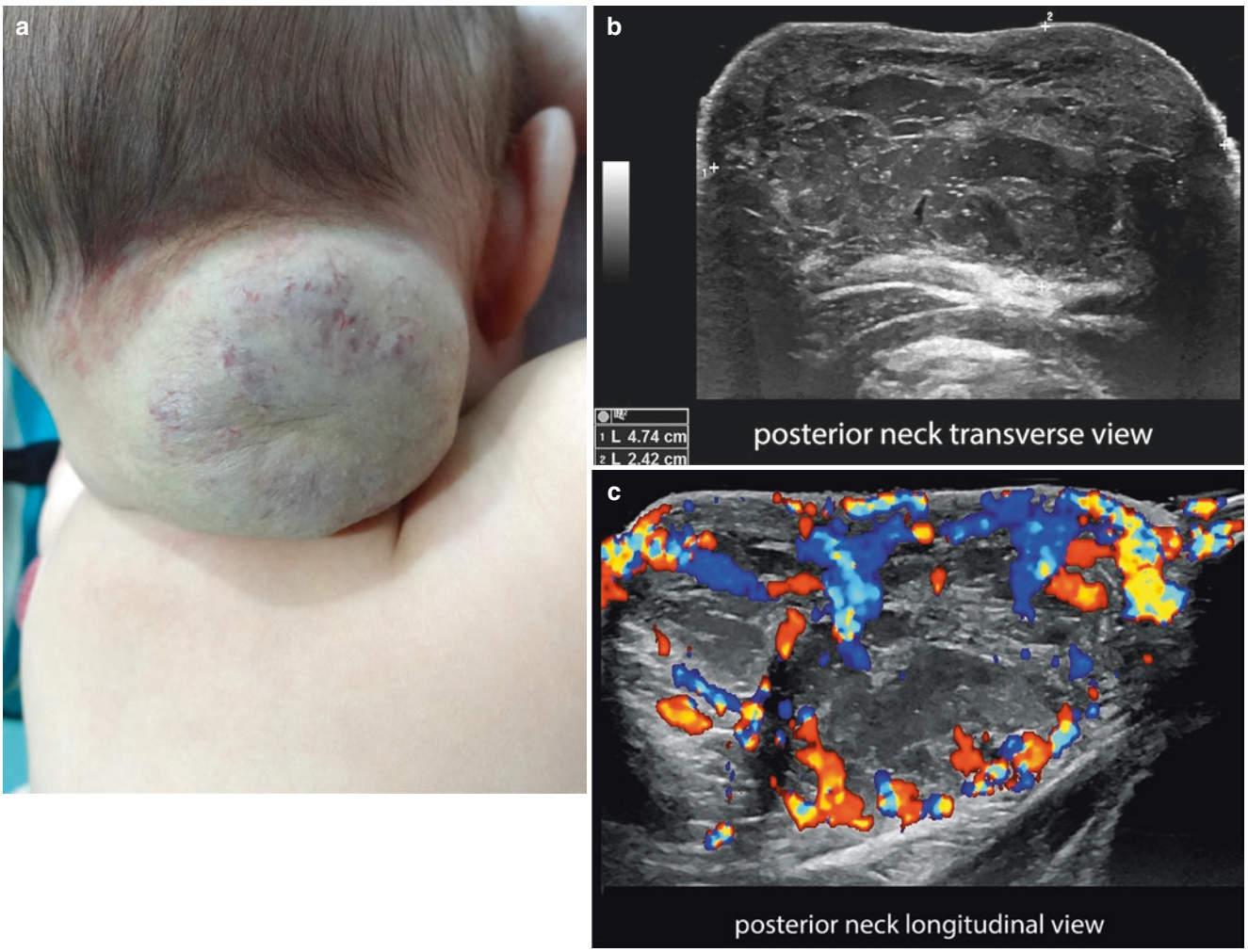

Fig. 4.11 Non-involuting congenital hemangioma (NICH) in a 3-month-old child. (**a**) Clinical image (posterior neck). (**b** and **c**) Greyscale and color Doppler ultrasound (**b**, transverse view; **c**, longitudinal view) shows 4.74-cm (transverse) × 2.4-cm (thickness) hypoechoic dermal and hypodermal exophytic, mass-like structure with anechoic tubular and lacunar areas. On color Doppler (**c**), there is prominent vascularity within the mass, comprising arterial and venous vessels without arteriovenous shunts. See Video 4.8.

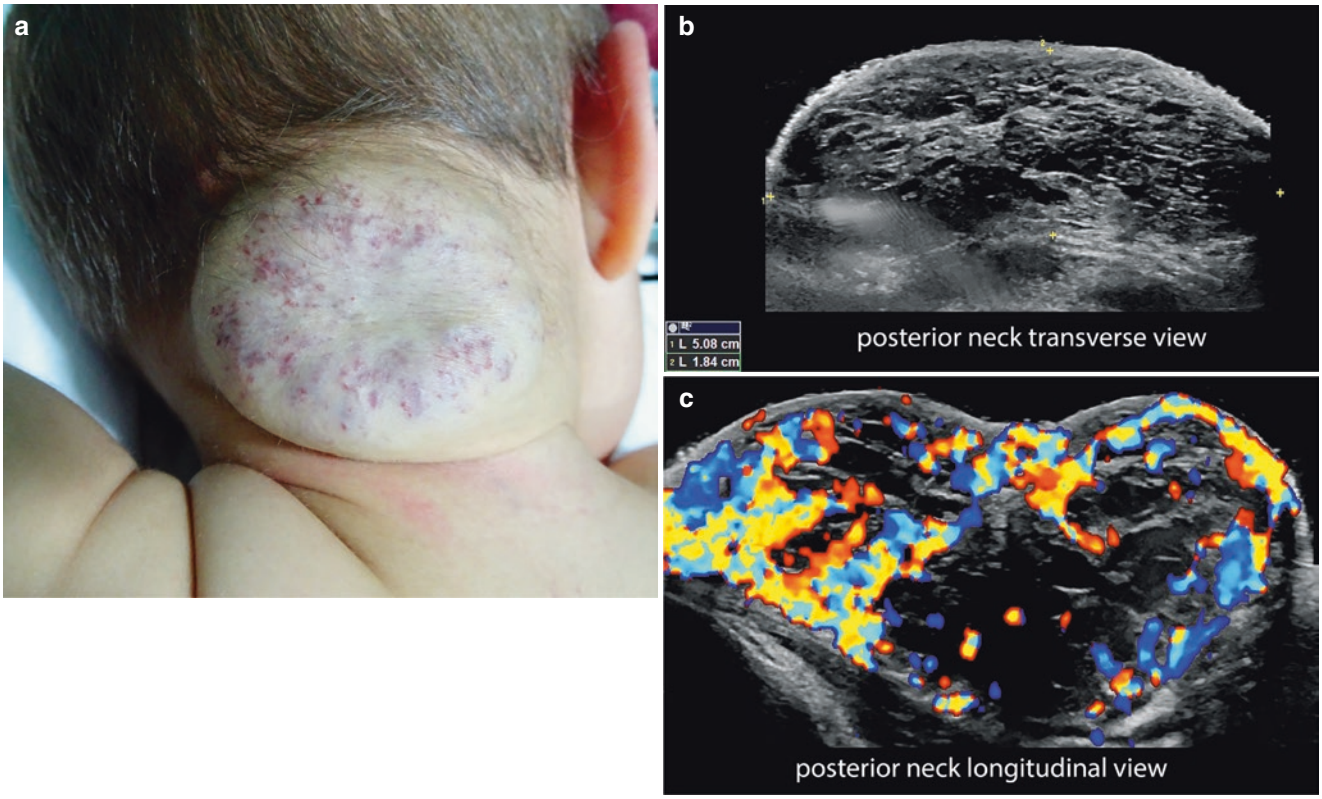

Fig. 4.12 Non-involuting congenital hemangioma (NICH). Follow-up at 1 year and 6 months of the same case as in Fig. 4.11. (**a**) Clinical image (posterior neck). (**b** and **c**) Greyscale and color Doppler ultrasound (**b**, transverse view; **c**, longitudinal view) show no significant changes in the diameter of the lesion, a 5.0-cm (transverse) × 1.8-cm (thickness) hypoechoic dermal and hypodermal exophytic, mass-like structure that maintains its anechoic tubular and lacunar areas. On color Doppler (**c**), there is still prominent vascularity within the mass with a similar pattern of arterial and venous vessels without arteriovenous shunts. See Video 4.9.

4.1.3.2 Synonyms

Pyogenic granuloma, lobular capillary hemangioma.

4.1.3.3 Key Sonographic Signs

- Exophytic or polypoid epidermal and dermal hypoechoic solid structure, when affecting the skin (Fig. 4.13; Video 4.10).
- In the nail bed, these tumors tend to show an ill-defined hypoechoic structure that displaces the nail plate upward. Erosion of the bony margin is not common, but in long-term cases usually associated with infection, irregularities and/or erosions of the underlying bony margin can be detected.
- Telangiectatic granuloma can also affect the epidermal and dermal layers of the periungual region, more commonly seen at the proximal nail fold.
- On color Doppler, these lesions show high vascularity with arterial and venous vessels, commonly presenting low velocities (Fig. 4.13) [12, 21].

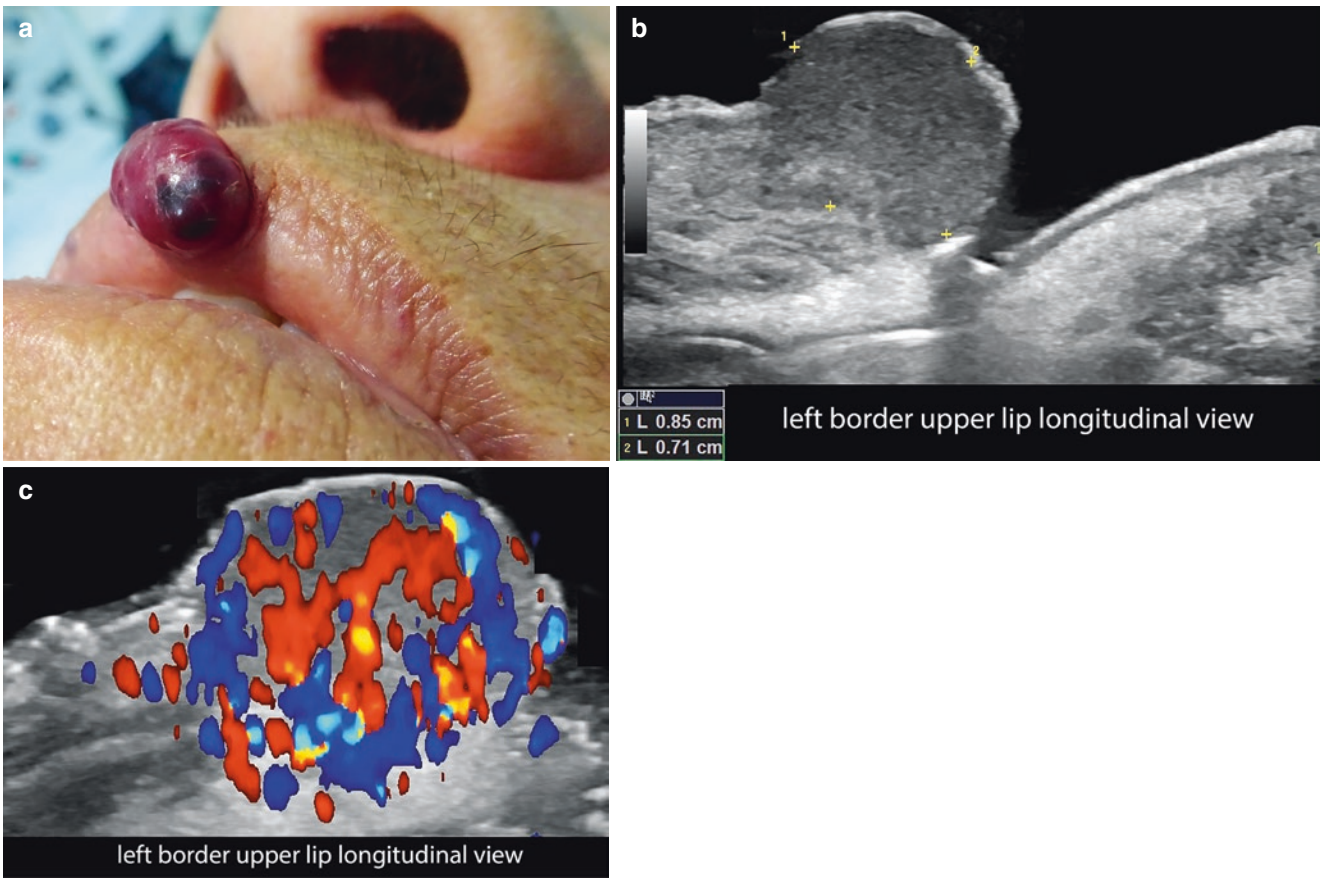

Fig. 4.13 Telangiectatic granuloma. (**a**) Clinical image of the lesion in the upper lip. (**b** and **c**) Greyscale and color Doppler ultrasound (longitudinal views; left border of the upper lip) demonstrates 8.5-mm (long) × 7.1-mm (thickness) exophytic, polypoid mass-like epidermal and dermal structure. On color Doppler, there is prominent and diffuse hypervascularity within the lesion. See Video 4.10.

4.1.4 Other Vascular Tumors

These include tufted angioma (TA) and kaposiform hemangioendothelioma (KHE), which present histological similarities and are positive for lymphatic endothelial markers D2–40 and Prox1 (Prospero homeobox protein 1). Both can be associated with consumptive coagulopathy, also called the Kasabach-Merritt phenomenon (thrombocytopenia, hemolytic anemia, and coagulation abnormalities). One of the main differences between these two tumors is that KHEs tend to infiltrate hypodermis and muscle [22, 23].

Among the borderline or locally destructive vascular tumors are KHE and other rare vascular tumors such as retiform hemangioendothelioma, composite hemangioendothelioma, and papillary intralymphatic angioendothelioma (Dabska tumor) [22–25].

The malignant vascular tumors include angiosarcoma and epithelioid hemangioendothelioma (EHE). Angiosarcomas are most commonly seen in the head, neck, and breast, but they can be seen in other corporal locations and can present after radiation or chronic lymphedema [26].

4.1.4.1 Cutaneous Kaposiform Hemangioendothelioma (KHE)

Definition

Locally aggressive endothelial proliferation that involves the skin and underlying layers [22, 23].

Key Sonographic Signs

- Ill-defined structure with heterogeneous echogenicity that usually involves dermis, hypodermis, and the underlying muscle layer.
- The vascularity tends to be prominent, with low-velocity arterial and venous vessels (Fig. 4.14).

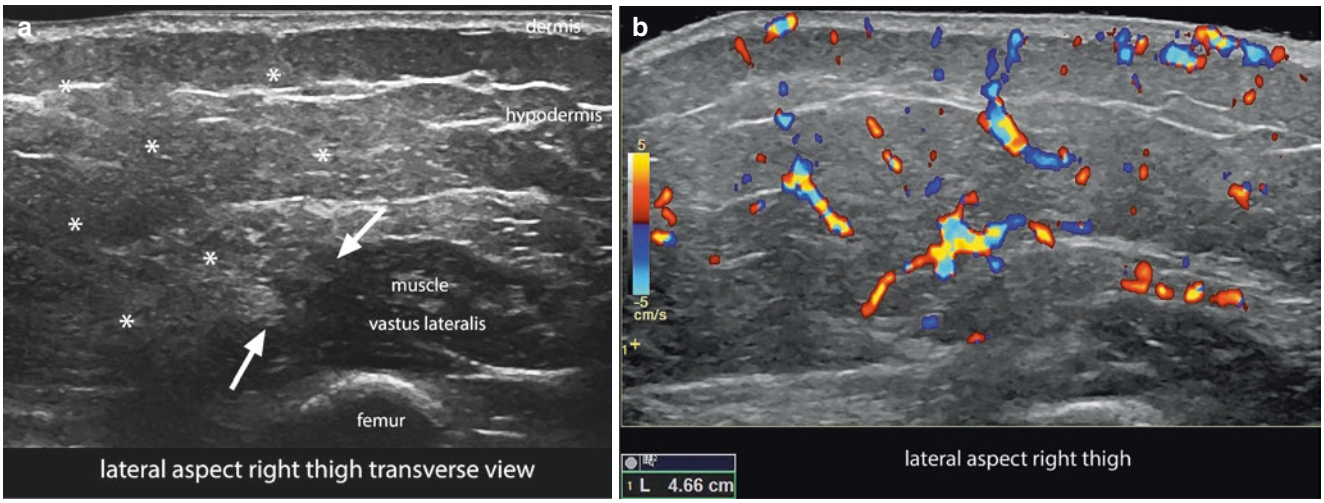

Fig. 4.14 Cutaneous kaposiform hemangioendothelioma (KHE). (**a** and **b**) Greyscale and color Doppler ultrasound (transverse views; lateral aspect of the right thigh) show ill-defined hyperechogenicity (*asterisks*) in the hypodermis, which involves the fascial layer and the surface of the lateral aspect of the vastus lateralis muscle. On color Doppler, there is asymmetric hypervascularity in the dermis and hypodermis, with tortuous and irregular vessels that also involve the surface of the lateral aspect of the vastus lateralis muscle.

4.1.4.2 Cutaneous Angiosarcoma

Definition

Malignant endothelial proliferation that affects the skin and deeper layers and can metastasize. The most common sites of presentation are the scalp, breast, and extremities; the most frequent site of metastasis is the lung. It can appear as single or multiple lesions, which can also present as satellites of the main lesion [12, 24–26].

Key Sonographic Signs

- Ill-defined hypoechoic or heterogeneous dermal and hypodermal solid mass with irregular or lobulated borders
- Involvement of deeper layers such as tendons, muscles, and bone can be detected.
- On color Doppler, prominent vascularity with low-velocity arterial and venous vessels can be seen in the whole tumor or in parts of the mass with irregular and tortuous vessels (Fig. 4.15).

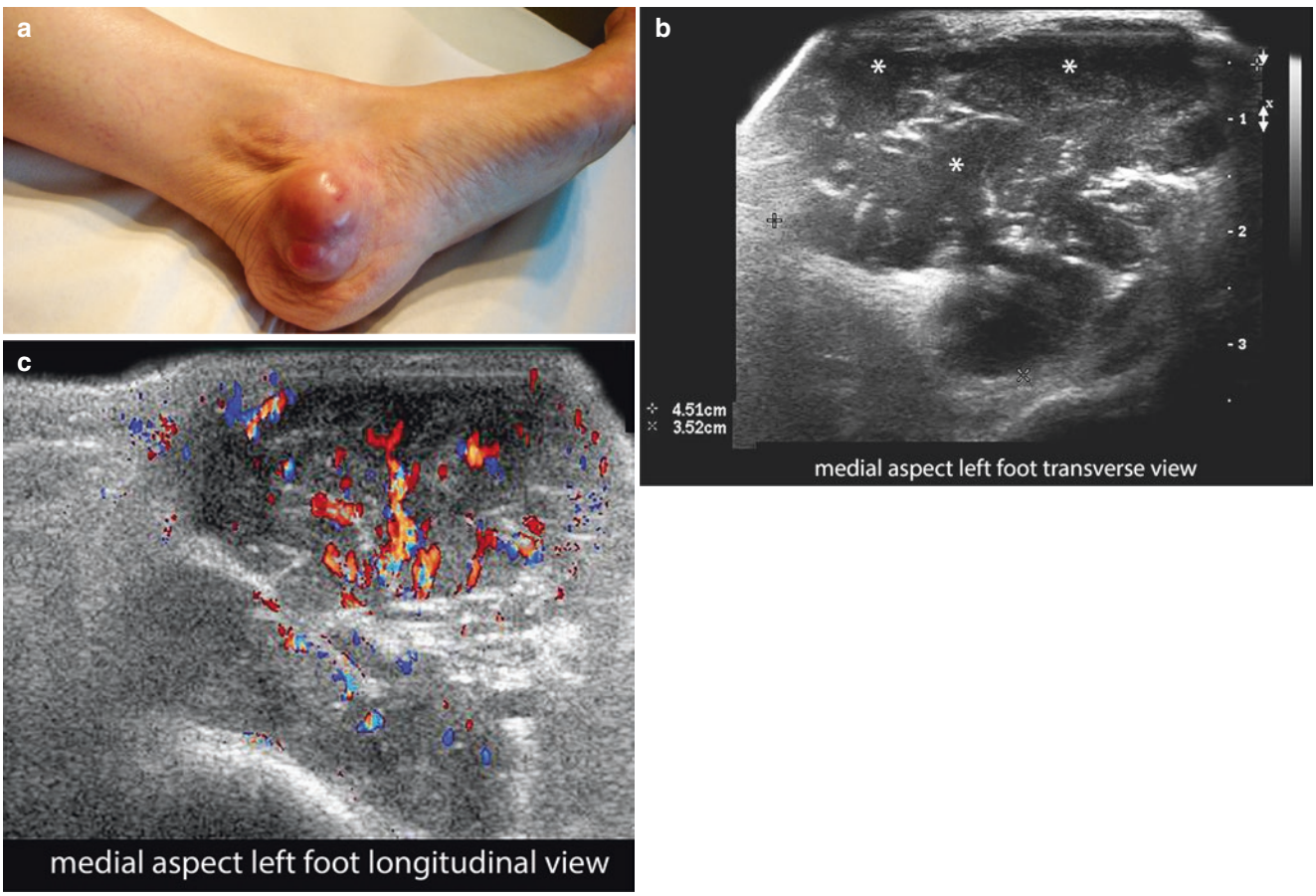

Fig. 4.15 Cutaneous angiosarcoma. (**a**) Clinical photograph of the mass in the medial aspect of the left foot. (**b** and **c**) Greyscale and color Doppler ultrasound (**b**, transverse view; **c**, longitudinal view) show 4.5-cm (transverse) × 3.5-cm (thickness) ill-defined dermal and hypodermal hypoechoic mass (*asterisks*) with some lobulated borders. On color Doppler (**c**), there is hypervascularity with irregular and tortuous vessels within the lesion.

4.2 Vascular Malformations

4.2.1 Definition

Error in the morphogenesis of the vessels, which generates dysplastic vascular channels. Vascular malformations (VMs) are commonly present at birth and grow slowly and proportionally with the child.

4.2.2 Classification

VMs can be classified according to the type of flow:

- High-flow
  - Arterial and communicating, with arteriovenous fistulas or shunts
  - Non-communicating arteriovenous tracts
- Low-flow (venous, capillary, lymphatic, or mixed)

These types are usually treated in different ways, so the sonographic support in the diagnosis can be relevant [1–3, 6, 8–10, 13, 27, 28].

4.2.3 Syndromes Associated to Vascular Malformations

Several congenital syndromes that present vascular malformations are listed in Table 4.1.

Capillary malformations are also present in salmon patch, hereditary hemorrhagic telangiectasia (HHT), cutis marmorata telangiectatica congenita, and cerebral cavernous malformation (CCM), and usually in the variants that show hyperkeratotic capillary malformations.

Venous malformations can be observed in familial VM cutaneomucosal (TIE2), blue rubber bleb nevus syndrome, and cerebral cavernous malformation (CCM).

Arteriovenous flow is seen in glomuvenous malformations, which are variants of VMs associated with glomus cells.

Lymphatic VM (LVM) can be separated into macrocystic, microcystic, or mixed. These are seen in Gorham-Stout disease, Nonne-Milroy syndrome, and primary hereditary lymphedema, as well as in several other, less frequent entities.

Table 4.1 Syndromes associated with vascular malformations

Syndrome	Types of vascular malformations
Klippel–Trenaunay	Low-flow vascular malformations (VMs)
M-CM or MCAP	Low-flow VM, usually capillary VM
CLOVES	Low- and/or high-flow VM
Proteus	Low-flow VMs
Parkes Weber	Low- and/or high-flow VM, usually capillary and/or arteriovenous
CM-AVM	Low- and/or high-flow VM
Sturge–Weber	Facial capillary VM
MICCAP	Low-flow VMs
Bannayan–Riley–Ruvalcaba	Low- and/or high- flow VM, usually capillary
SOLAMEN	High-flow VM
Maffucci	Low-flow VMs, usually venous VM
Servelle–Martorell	Low-flow VMs, usually venous VM

CLOVES congenital, lipomatous, overgrowth, vascular malformations, epidermal nevi and spinal/skeletal anomalies and/or scoliosis, *CM-AVM* capillary malformation-arteriovenous malformation, *MCAP* macrocephaly-capillary malformation, *MICCAP* microcephaly-capillary malformation, *SOLAMEN* segmental overgrowth, lipomatosis, arteriovenous malformation and epidermal nevus

4.2.4 Key Sonographic Signs

- Network of tortuous, anechoic, tubular structures or lacunar areas
- Lack of mass-like appearance
- VMs can be classified according to the shape of the curve in the spectral analysis of the color Doppler evaluation (Figs. 4.16, 4.17, 4.18, 4.19, 4.20, 4.21, and 4.22, Videos 4.11, 4.12, 4.13, and 4.14). Thus, arterial VMs will show a curve with systolic and diastolic peaks, venous VMs will present a curve with monophasic flow, and arteriovenous VMs will show a mix of arterial and venous curves plus some arteriovenous shunts or arterialized venous flow. Lymphatic VMs commonly do not show continuous flow. Flow is not detected in capillary VMs because of the very slow velocity and the small size of these capillary vessels.
- In some cases, a combination of different types of VMs can be seen. The most common mixes are venous and arterial, venous and lymphatic, and venous and capillary.
- Venous VMs are usually compressible with the probe and can present hyperechoic calcifications (called *phleboliths*) in some areas.
- VMs commonly do not show significant changes in size, echogenicity, and vascularity, and they tend to grow proportionally with the child. They may present thrombosis in some areas, which is more commonly seen with venous VMs. Therefore, some of the vascular channels can be dilated, hypoechoic, non-compressible, and show no presence of blood flow on color Doppler.
- Keep in mind that blood flow is usually detected on color Doppler when the velocity of the vessels is at least 2 cm/s.

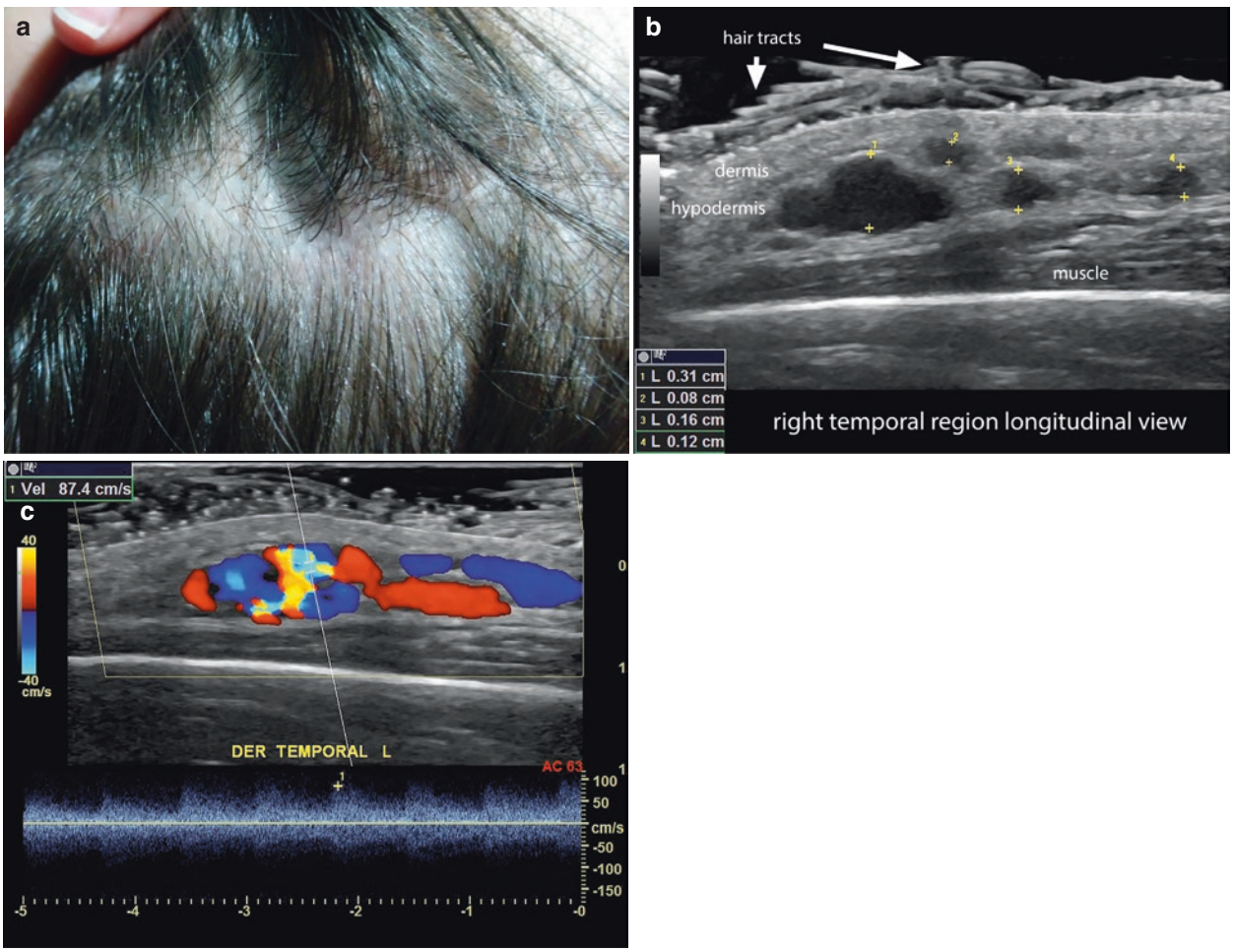

Fig. 4.16 High-flow arterial vascular malformation. (**a**) Clinical image of the right temporal region in the scalp. (**b**) Greyscale ultrasound (right temporal region, longitudinal view) presents multiple anechoic, lacunar, hypodermal communicating spaces and tracts (between markers), which vary in their thickness between 0.8 and 3.1 mm. (**c**) Color Doppler spectral curve analysis shows high peak systolic arterial velocity (87.4 cm/s) within the network of vessels. A feeding arterial vessel to the network of vessels coming from the right temporal artery was also detected on this examination. See Video 4.11.

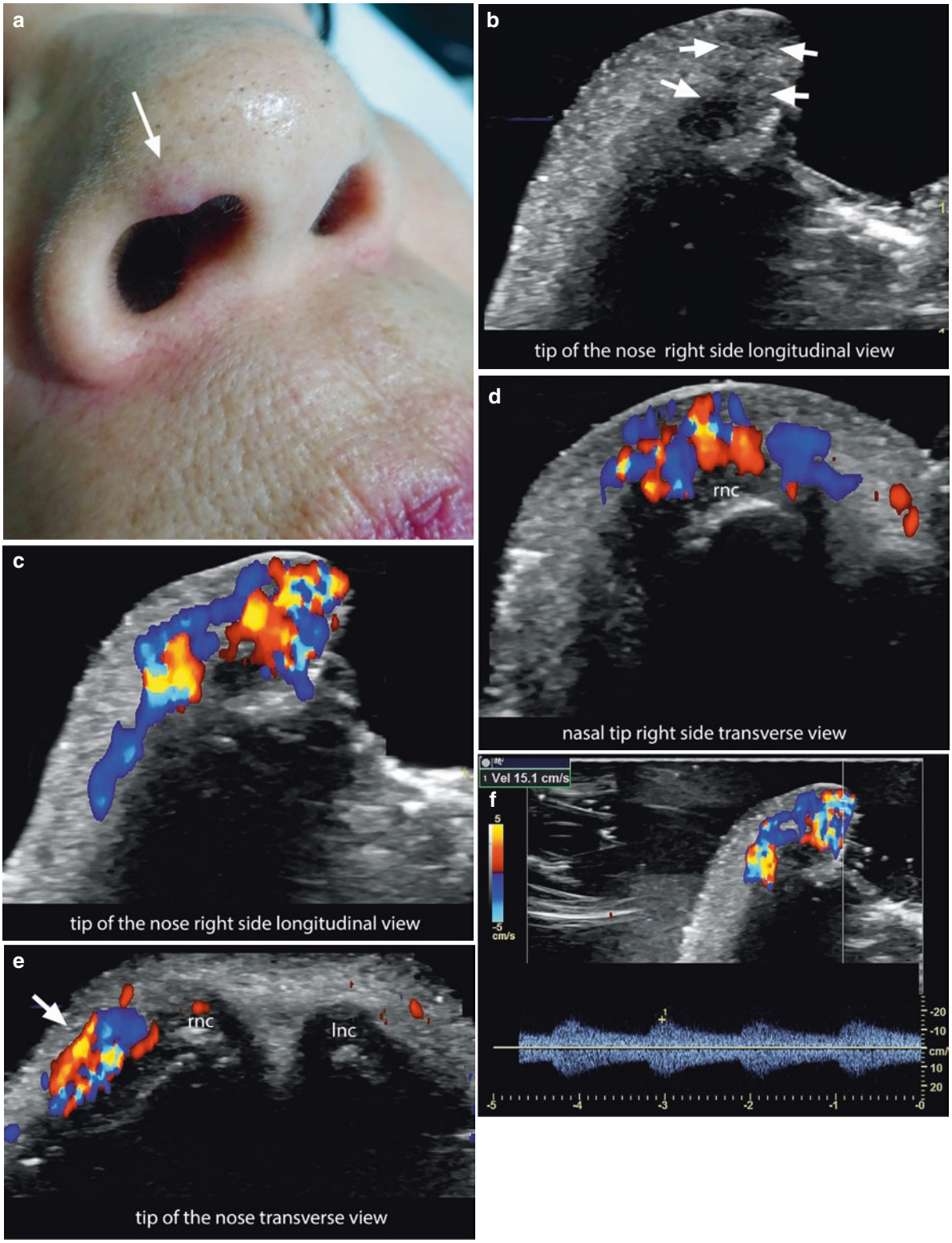

Fig. 4.17 High-flow arterial vascular malformation. (**a**) Clinical image shows a lesion (*arrow*) in the right side of the tip of the nose. (**b**) Greyscale ultrasound; (**c**–**e**) Color Doppler ultrasound. (**f**) Spectral curve analysis of the blood flow in the same region. An ill-defined, hypoechoic dermal area in Greyscale (**b**, *arrows*) clearly becomes a network of tortuous dermal vessels on color Doppler (**c**, longitudinal view; **d**, transverse view). The dermal hypervascularity at the anterior aspect of the right nostril involves the surface of the right alar nasal cartilage (**c**–**e**). In the spectral curve analysis (**f**), the peak systolic velocity is 15.1 cm/s, which is a high velocity for the dermis. Notice that there is no mass-like structure between the vessels. *rnc* right alar nasal cartilage, *lnc* left alar nasal cartilage. See Video 4.12.

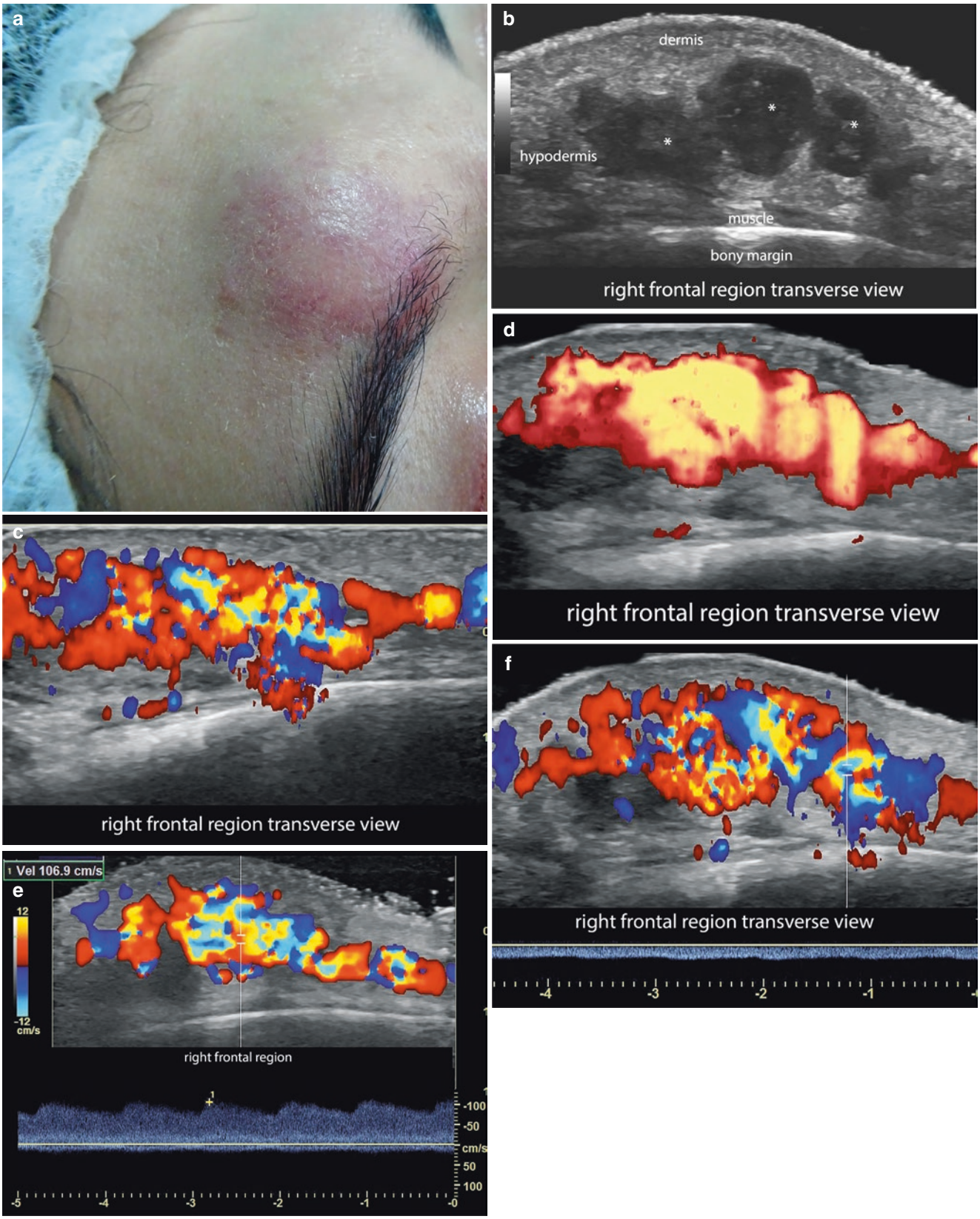

Fig. 4.18 High-flow arteriovenous vascular malformation. (**a**) Clinical photograph of the lesion in the right frontal region. (**b**) Greyscale ultrasound (transverse view) demonstrates hypoechoic, oval-shaped hypodermal structures (*asterisks*) and increased echogenicity of the hypodermis. Color Doppler (**c**) and power Doppler (**d**) (transverse views) show a network of hypodermal vessels in this region. (**e** and **f**) Spectral curve analyses of the blood flow demonstrate high-velocity arterialized venous flow in the center of the lesion, which reaches 106.9 cm/s (**e**); other parts show venous monophasic flow. See Video 4.13.

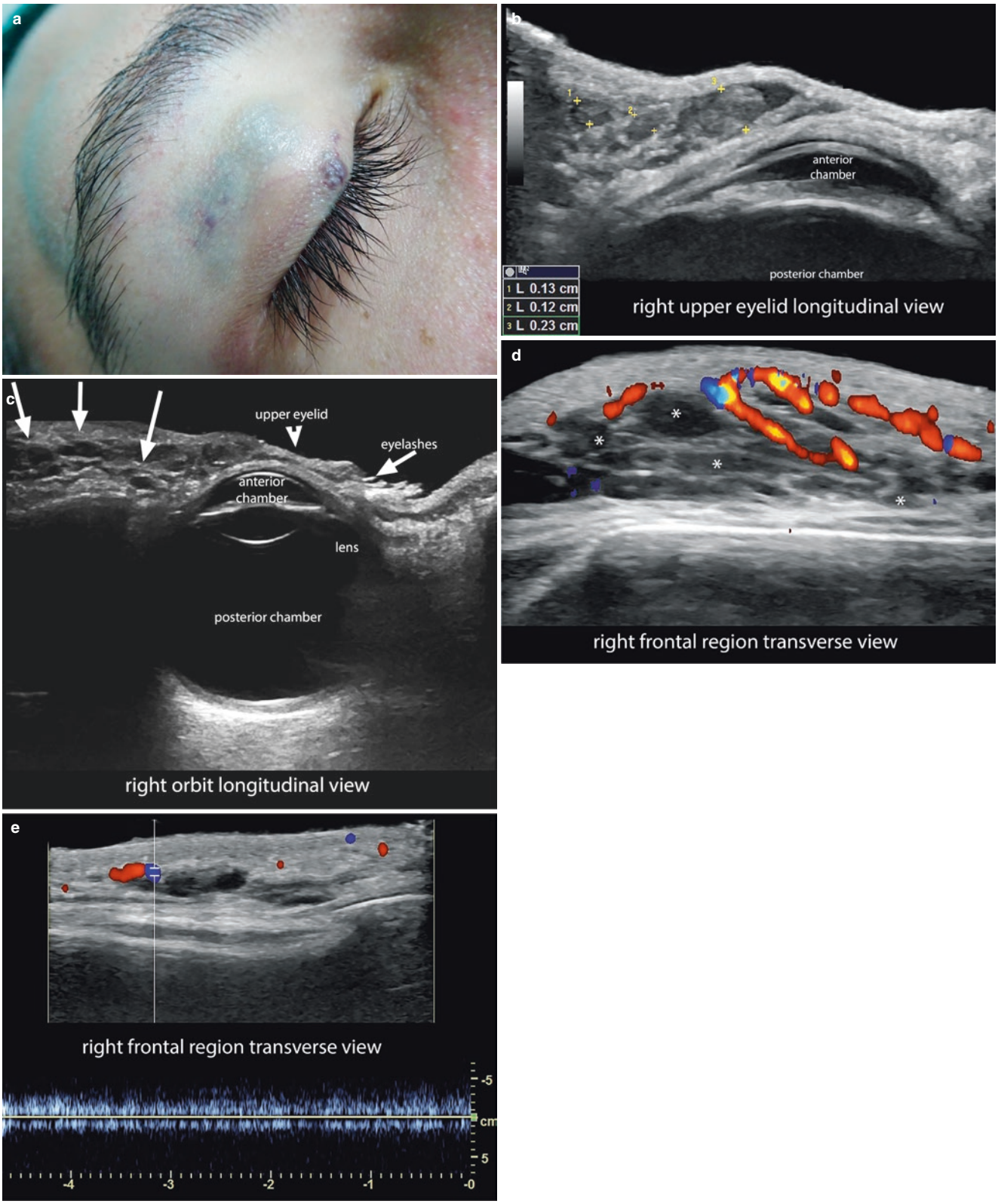

Fig. 4.19 Low-flow venous vascular malformation with partial thrombosis. (**a**) Clinical image of the lesion in the upper eyelid. (**b** and **c**) Greyscale images (longitudinal views; **b**, focused on the eyelid; **c**, focused on the orbit) show multiple hypoechoic and anechoid lacunar and tubular structures (between markers in **b**) that involve the orbicularis muscle of the right upper eyelid and its frontal part, as well as the posterior aspect of the upper eyelid on the same side. These lacunar and tubular structures measure between 1.2 and 2.3 mm in thickness (**b**); they extend to the hypodermis of the right frontal region (**c**, *arrows in the left part of the image*). The hypoechogenicity in some of these structures is suggestive of partial thrombosis. (**d**) Color Doppler ultrasound (transverse view) shows no signs of vascularity in some of these tubular and lacunar structures (*asterisk*). (**e**) Spectral curve analysis of some of the vessels demonstrates low-velocity venous flow.

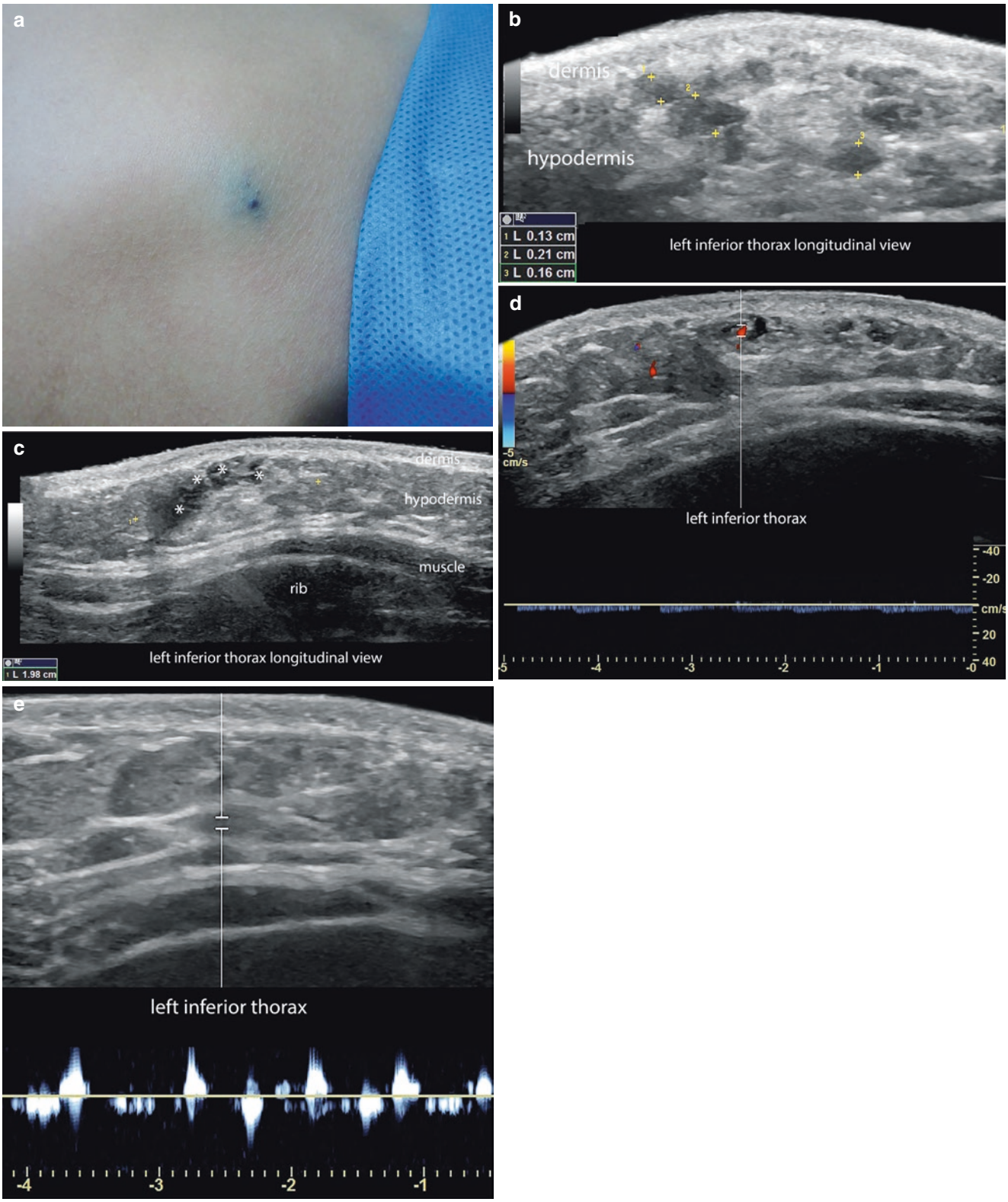

Fig. 4.20 Low-flow venous vascular malformation. (**a**) Clinical image of the lesion in the lower part of the left side of the thorax. (**b** and **c**) Greyscale images (longitudinal views; **b**, zoom in; **c**, panoramic view) show multiple hypoechoic and anechoid hypodermal lacunar and tubular structures (between markers in **b**; *asterisks* in **c**). These lacunar and tubular structures measure between 1.3 and 2.1 mm in thickness (**b**). The hypoechogenicity in some of these structures is suggestive of sites with partial thrombosis. (**d** and **e**) Spectral curve analysis of the flow demonstrates lack of detectable flow in some parts, but a low-velocity flow appears with the compression of these structures (**e**). See Video 4.14.

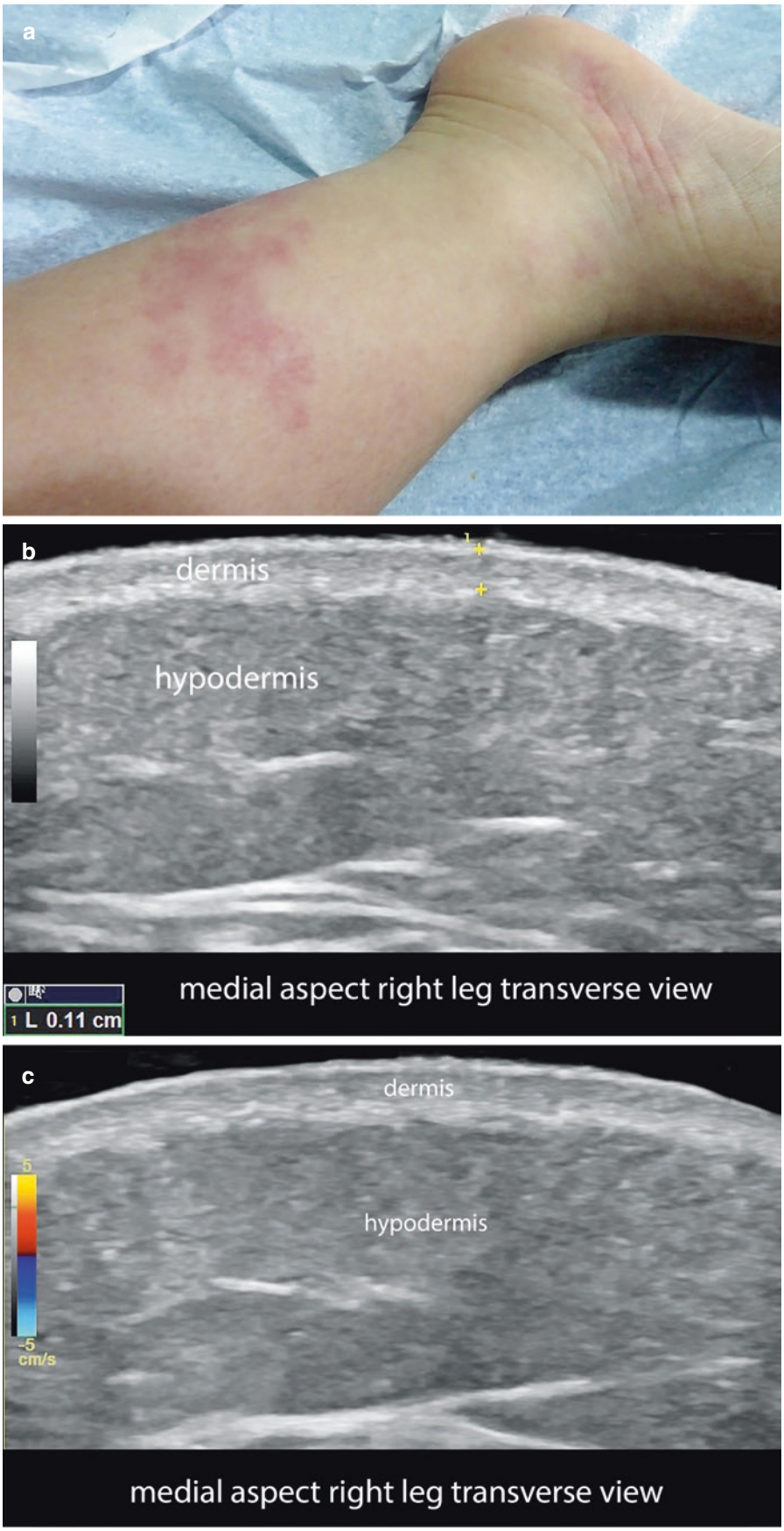

Fig. 4.21 Low-flow capillary vascular malformation. (**a**) Clinical photograph of the lesion in the medial aspect of the right leg and foot. (**b** and **c**) Greyscale and color Doppler ultrasound (transverse views) show slightly decreased echogenicity of the upper dermis (**b**), but neither signs of abnormal thickness or echogenicity in the deeper layers (**b**) nor signs of hypervascularity (**c**) are detected in the region.

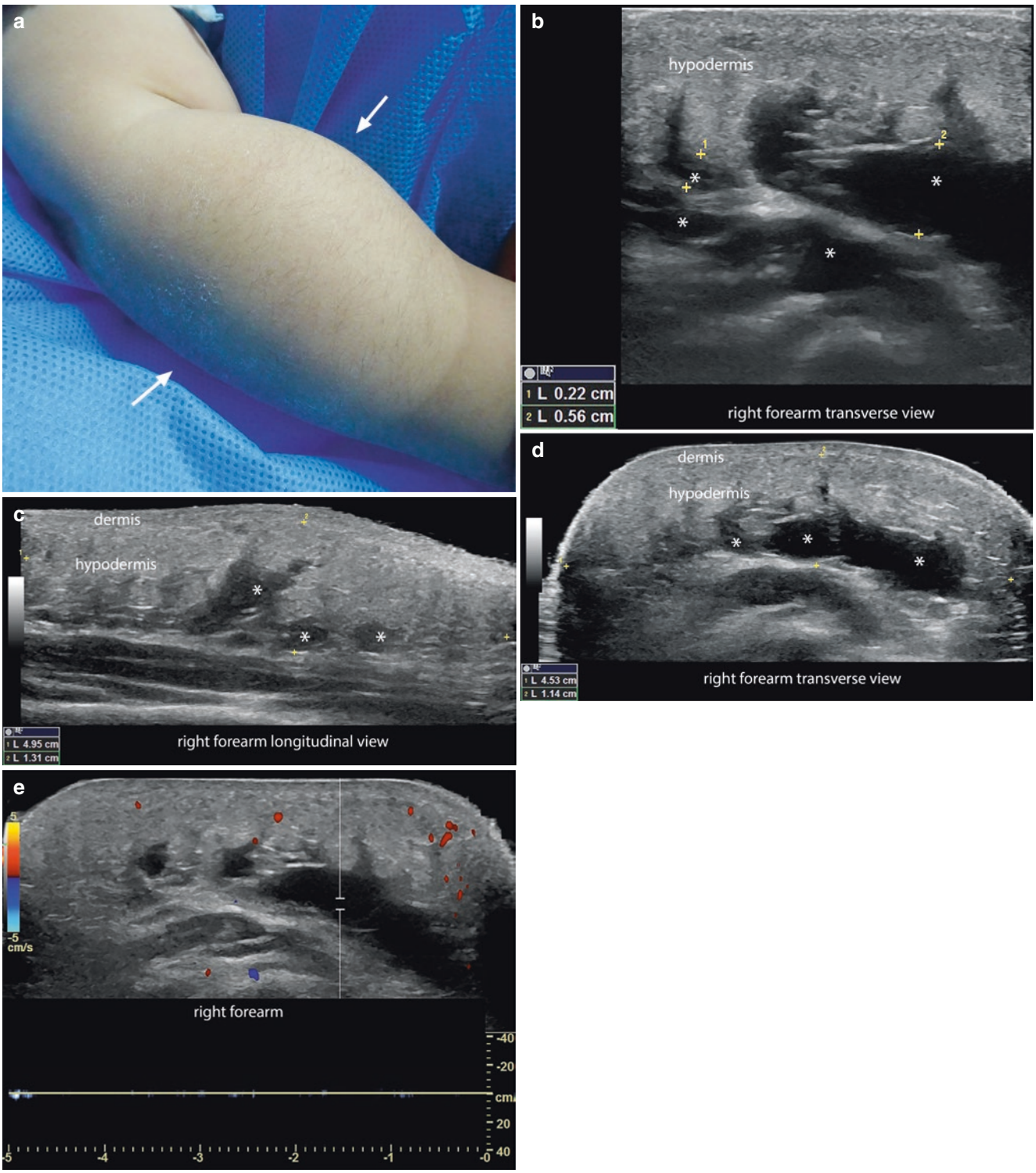

Fig. 4.22 Low-flow lymphatic vascular malformation. (**a**) Clinical image that shows swelling of the right forearm. (**b**–**d**) Greyscale ultrasound. A longitudinal zoom-in view (**b**) and transverse panoramic view (**c**) demonstrate multiple anechoic and irregular hypodermal tubular and lacunar anechoic fluid-filled spaces (*asterisks*), which vary in thickness between 2.2 and 5.6 mm. These spaces are located in an area that measures 5.0 cm (long) × 1.3 cm (thickness) × 4.5 cm (transverse). Notice the increased echogenicity and thickness of the regional hypodermis. (**e**) The spectral curve analysis shows no detectable flow within these spaces.

4.3 Provisionally Unclassified Vascular Anomalies

4.3.1 Angiokeratoma

4.3.1.1 Definition

Benign proliferation of dilated capillary blood vessels in the upper dermis and hyperkeratosis. The most common form of presentation is a solitary reddish or purple, warty-like lesion in one corporal region, but it can appear as multiple lesions or as a diffuse form of presentation, which can be associated with Fabry disease. Common sites of involvement are the limbs or vulvar and scrotal regions, but it can affect other sites [12, 29]. Recently, an association of angiokeratomas with cavernous vascular malformations of the brain has been reported [30]. Therefore, a brain imaging study such as MRI could be desirable in these cases.

4.3.1.2 Key Sonographic Signs

- Band-like epidermal and dermal structure
- Thickening, undulation, and irregularities of the epidermis
- Thickening and decreased echogenicity of the dermis (Fig. 4.23)
- On color Doppler, tendency to show hypovascularity

4.3.2 Verrucous Hemangioma

4.3.2.1 Definition

Benign proliferation of dilated capillary blood vessels in the dermis and hypodermis, with a variable degree of hyperkeratosis of the epidermis. Verrucous hemangioma (VH) is similar to angiokeratoma but deeper [12, 31].

Fig. 4.23 Angiokeratoma. (**a**) Clinical image in the medial aspect of the distal part of the thigh. (**b** and **c**) Greyscale and color Doppler (longitudinal views) demonstrate thickening and undulation of the epidermis and decreased echogenicity of the upper dermis. On color Doppler, the lesion appears hypovascular.

4.3.2.2 Key Sonographic Signs

- Variable degree of thickening, undulation and irregularities of the epidermis.
- Thickening and decreased echogenicity of the dermis (Fig. 4.24).
- Ill-defined hyperechogenicity of the underlying hypodermis.
- On color Doppler, VH tend to show hypovascularity due to their slow-flow capillary vessels.

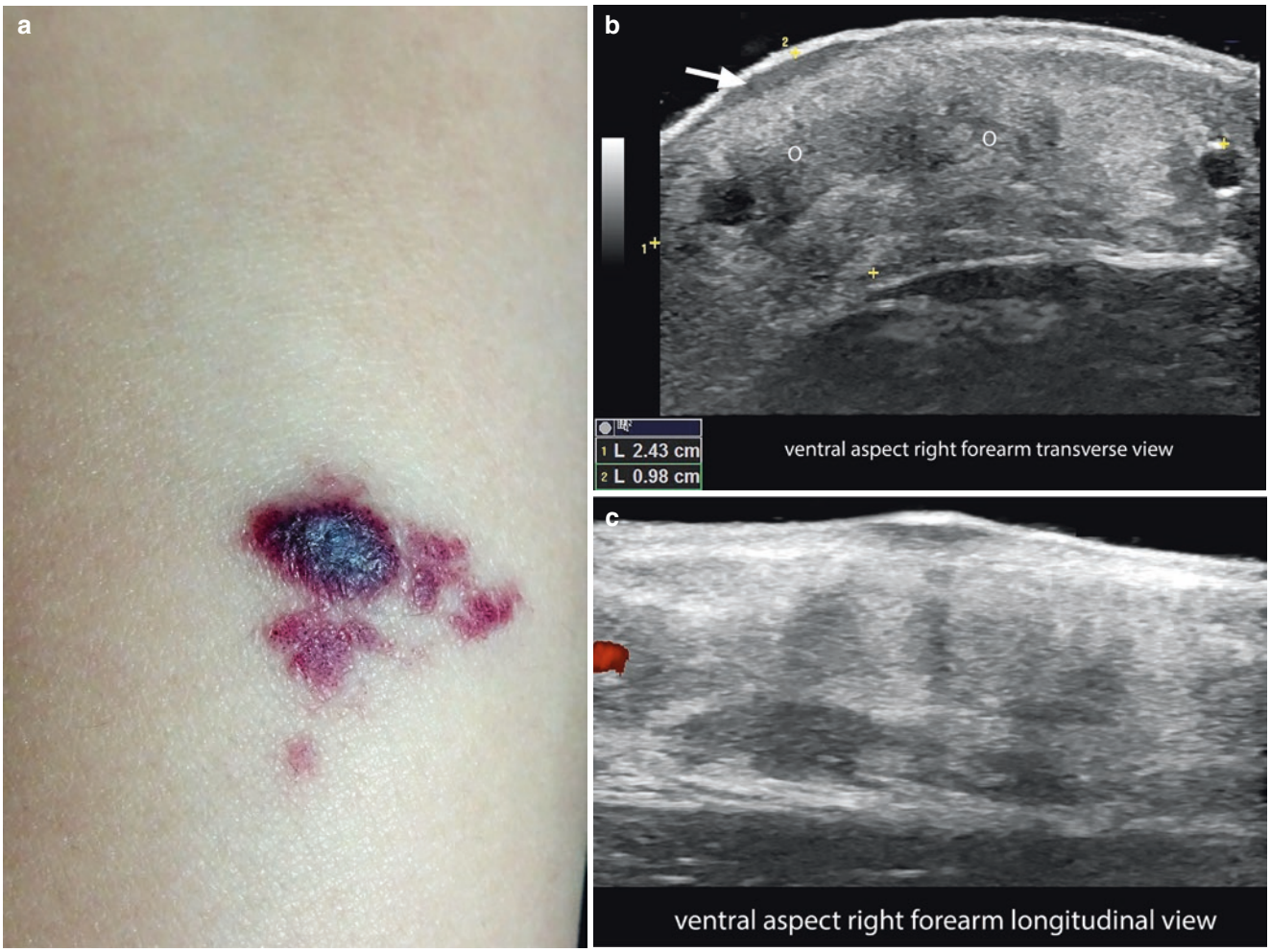

Fig. 4.24 Verrucous hemangioma. (**a**) Clinical photograph. (**b** and **c**) Greyscale (transverse view) and color Doppler (longitudinal view) ultrasound of the ventral aspect of the right forearm shows thickening and mixed echogenicity (*o*) of the dermis and hypodermis, with upward displacement of the epidermis, decreased echogenicity of the upper dermis (*arrow*) and a more hyperechoic and heterogeneous hypodermis. The area of abnormality of the echostructure measures 2.4 cm (transverse) × 1.0 cm (thickness). On color Doppler (**c**), no signs of hypervascularity are detected in this region.

References

1. International Society for the Study of Vascular Anomalies. ISSVA classification for vascular anomalies (Approved at the 20th ISSVA Workshop, Melbourne, April 2014). http://www.issva.org/UserFiles/file/Classifications-2014-Final.pdf. Accessed 4 Dec 2017.
2. Jahnke MN. Vascular lesions. Pediatr Ann. 2016;45:e299–305.
3. Garzon MC, Weitz N, Powell J. Vascular anomalies: differential diagnosis and mimickers. Semin Cutan Med Surg. 2016;35:170–6.
4. Smith CJF, Friedlander SF, Guma M, Kavanaugh A, Chambers CD. Infantile hemangiomas: an updated review on risk factors, pathogenesis, and treatment. Birth Defects Res. 2017;109:809–15.
5. Hoeger PH, Colmenero I. Vascular tumours in infants. Part I: benign vascular tumours other than infantile haemangioma. Br J Dermatol. 2014;171:466–73.
6. Merrow AC, Gupta A, Patel MN, Adams DM. 2014 revised classification of vascular lesions from the international society for the study of vascular anomalies: radiologic-pathologic update. Radiographics. 2016;36:1494–516.
7. Miller DD, Gupta A. Histopathology of vascular anomalies: update based on the revised 2014 ISSVA classification. Semin Cutan Med Surg. 2016;35:137–46.
8. Steiner JE, Drolet BA. Classification of vascular anomalies: an update. Semin Interv Radiol. 2017;34:225–32.
9. Wortsman X. Common applications of dermatologic sonography. J Ultrasound Med. 2012;31:97–111.
10. Wortsman X. Ultrasound in dermatology: why, how and when? Semin Ultrasound CT MR. 2013;34:177–95.
11. Kutz AM, Aranibar L, Lobos N, Wortsman X. Color Doppler ultrasound follow-up of infantile hemangiomas and peripheral vascularity in patients treated with propranolol. Pediatr Dermatol. 2015;32:468–75.
12. Wortsman X, Carreño L, Morales C. Cutaneous vascular tumors. In: Wortsman X, Jemec GBE, editors. Dermatologic ultrasound with clinical and histologic correlations. New York: Springer; 2013. p. 235–48.
13. Peer S, Wortsman X. Hemangiomas and vascular malformations. In: Wortsman X, Jemec GBE, editors. Dermatologic ultrasound with clinical and histologic correlations. New York: Springer; 2013. p. 183–234.
14. Wortsman X, Alfageme F, Roustan G, Arias-Santiago S, Martorell A, Catalano O, et al. Guidelines for performing dermatologic ultrasound examinations by the DERMUS group. J Ultrasound Med. 2016;35:577–80.
15. He L, Huang G. Spectral Doppler ultrasound for predicting long-term response to topical timolol in children with infantile hemangioma. J Clin Ultrasound. 2017;45:480–7.
16. García-Martínez FJ, Muñoz-Garza FZ, Hernández-Martín A. [Ultrasound in pediatric dermatology]. Actas Dermosifiliogr. 2015;106(Suppl 1):76–86.
17. Amouri M, Mesrati H, Chaaben H, Masmoudi A, Mseddi M, Turki H. Congenital hemangioma. Cutis. 2017;99:E31–3.
18. Wortsman X, Wortsman J, Aranibar L. Congenital diseases of the skin. In: Wortsman X, Jemec GBE, editors. Dermatologic ultrasound with clinical and histologic correlations. New York: Springer; 2013. p. 39–72.
19. Chen CP, Chen CY, Chang TY, Yang HY, Chen YN, Chen SW, Wang W. Prenatal imaging findings of a rapidly involuting congenital hemangioma (RICH) over right flank in a fetus with a favorable outcome. Taiwan J Obstet Gynecol. 2016;55:745–7.
20. Koo MG, Lee SH, Han SE. Pyogenic granuloma: a retrospective analysis of cases treated over a 10-year. Arch Craniofac Surg. 2017;18:16–20.
21. Silva-Feistner M, Ortiz E, Alvarez-Véliz S, Wortsman X. Amelanotic subungual melanoma mimicking telangiectatic granuloma: clinical, histologic, and radiologic correlations. Actas Dermosifiliogr. 2017;108:785–7.
22. Croteau SE, Gupta D. The clinical spectrum of kaposiform hemangioendothelioma and tufted angioma. Semin Cutan Med Surg. 2016;35:147–52.
23. Ryu YJ, Choi YH, Cheon JE, Kim WS, Kim IO, Park JE, Kim YJ. Imaging findings of kaposiform hemangioendothelioma in children. Eur J Radiol. 2017;86:198–205.
24. Colmenero I, Hoeger PH. Vascular tumours in infants. Part II: vascular tumours of intermediate malignancy [corrected] and malignant tumours. Br J Dermatol. 2014;171:474–84.
25. Nozaki T, Matsusako M, Mimura H, Osuga K, Matsui M, Eto H, et al. Imaging of vascular tumors with an emphasis on ISSVA classification. Jpn J Radiol. 2013;31:775–85.
26. Gaballah AH, Jensen CT, Palmquist S, Pickhardt PJ, Duran A, Broering G, Elsayes KM. Angiosarcoma: clinical and imaging features from head to toe. Br J Radiol. 2017;90:20170039.
27. Sun RW, Tuchin VV, Zharov VP, Galanzha EI, Richter GT. Current status, pitfalls and future directions in the diagnosis and therapy of lymphatic malformation. J Biophotonics. 2017. https://doi.org/10.1002/jbio.201700124. [Epub ahead of print].
28. Acord M, Srinivasan AS, Cahill AM. Percutaneous treatment of lymphatic malformations. Tech Vasc Interv Radiol. 2016;19:305–11.
29. Lidove O, Jaussaud R, Aractingi S. Dermatological and soft-tissue manifestations of Fabry disease: characteristics and response to enzyme replacement therapy. In: Mehta A, Beck M, Sunder-Plassmann G, editors. Fabry disease: perspectives from 5 years of FOS, chap. 24. Oxford: Oxford PharmaGenesis; 2006.
30. Whitworth WW, Hick RW, Nelson KC, Sidhu-Malik NK. Cerebral cavernous malformations associated with cutaneous angiokeratomas and hemangiomas. Cutis. 2015;96:329–32.
31. Singh J, Sharma P, Tandon S, Sinha S. Multiple verrucous hemangiomas: a case report with new therapeutic insight. Indian Dermatol Online J. 2017;8:254–6.